3

Current State of Art in Earthquake Prediction, Typical Precursors and Experience in Earthquake Forecasting at Sakhalin Island and Surrounding Areas

I.N. Tikhonov[1] and M.V. Rodkin[1,2]
[1]*Institute of Marine Geology and Geophysics FEB RAS, Yuzhno-Sakhalinsk*
[2]*International Institute of Earthquake Prediction Theory and Mathematical Geophysics RAS, Moscow*
Russia

1. Introduction

Despite of over a century of scientific effort, the understanding in earthquake forecasting remains immature. Moreover, even the theoretical possibility of earthquake forecasting is debatable. Especially problematic is a possibility of an effective short- and intermediate-term earthquake forecasting. The aim of this paper is to present the new evidence in support of possibility of the short- and intermediate-term earthquake forecasting. This possibility is shown through the discussion of seismic regime in the generalized vicinity of strong earthquake and through the description of an experience in an earthquake forecasting in the case of the Sakhalin Island and the surrounding areas.

USGS/NEIC catalog and Harvard seismic moments catalog are used to construct the generalized space–time vicinity of strong (M7+) earthquake to reveal the robust typical long-, intermediate, and short-term precursor anomalies. The very essential increase in available information resulted from this procedure gives possibility to detail the character of precursors of strong earthquake. The typical parameters of the fore- and aftershock cascades were detailed. A few other revealed precursory anomalies indicate the development of softening in the source area of a strong earthquake. The set of the precursory anomalies indicates the approaching of a strong event quite definitely. Thus one can conclude that the effective short- and intermediate-term earthquake forecasting appears to be possible in the case of essential increase of volume of statistical information available for the forecasting.

The current state of art in the earthquake forecasting is illustrated by the case of experience in the earthquake forecasting for the Sakhalin Island and the surrounding areas performed in the Institute of Marine Geology and Geophysics of the Far East Branch of the Russian Academy of Science, Yuzhno-Sakhalinsk, Russia. Four examples of successful prognosis (three of them performed in a real time), and one false alarm took place. Thus, despite the evident deficient in available information the results of forecasting appear to be encouraging

enough. In any case they are much better than they could be in the case if the seismic roulette model would be valid.

In the early 1980s a few examples of successful earthquake prognosis were known, and the final successes in decision of the problem of earthquake prognosis seemed to be close. But the substantial increase in a number of different sensors used in earthquake monitoring, and the corresponding increase in available information didn't improve the quality of prognosis. The situation was discussed widely in the 90s, and the dominant opinion elaborated by the world scientific community was quite pessimistic. An earthquake generating system was found to be very unstable. A minor change in parameters of such systems can significantly change their evolution; as a result an effective prognosis of behavior of such systems is impossible. Thus an earthquake prognosis was declared to be impossible (Geller, 1997; Geller et al., 1997; Kagan, 1997; and references herein). Despite of this dominating opinion a few groups of researchers have continued their investigations in earthquake forecasting. First of all the effectiveness of the suggested earlier algorithms of strong earthquake prediction was tested in real time. The results of the use of the M8 and Mendocino Scenario algorithms suggested earlier in (Keilis-Borok & Kossobokov, 1986, 1990; Kossobokov, 1986) were examined during more than twenty years. It was shown that the results of prognosis were significantly better than it could be in case of a seismic roulette procedure (Shebalin, 2006; Kossobokov, 2005). However neither these algorithms nor the other ones tested at shorter time intervals (Sobolev et al., 1999; Papazachos, 2005; Zavyalov, 2006; and others) showed results quite suitable for practical use. There were substantial probabilities to miss an earthquake or declare false alarm.

Low efficiency of earthquake prediction is connected to extremely irregular character of seismic regime. Due to the high level of irregularity of seismic regime parameters of earthquake precursors are vague, and even the very existence of precursor phenomena remains debatable. As a result in the absence of well known precursors any algorithm of forecasting based on the use of these precursors could hardly be very effective.

Thus verification of used precursor phenomena is an urgent problem. A precursory process and occurrence of large earthquake is commonly treated as an example of critical phenomenon (Akimoto & Aizawa, 2006; Bowman et al., 1998; Keilis-Borok & Soloviev, 2003; Malamud et al., 2005; Nonlinear …, 2002; Sornette, 2000; etc.). Many of the precursors used currently, such as development of foreshock cascade, an increase in correlation length, and an abnormal clustering of earthquakes, are expected to occur in critical processes. Moreover, some of these precursors came in the use because the process of strong earthquake occurrence is treated in terms of the critical phenomenon model. In this situation a natural question may arise: to what extent are such model processes really typical of scenarios of occurrence of large earthquake? Romashkova and Kossobokov (2001) have considered the evolution of foreshock and aftershock activity in the vicinities of eleven strong earthquakes occurring from 1985 to 2000. This examination has not supported the universality of power-law growth in foreshock activity toward the moment of a large earthquake. It also turned out that the aftershock sequences in a number of cases differ significantly from the Omori law. As a result it was hypothesized (Romashkova & Kossobokov, 2001; Kossobokov, 2005) that scenarios of aftershock sequences deviating from the Omori law can exist.

It seems natural to ask whether the observed deviations of the seismic process from the theoretically expected universal scenario have a stochastic nature or different scenarios can

be put into effect in different foreshock and aftershock sequences. The answer to that question can be obtained by investigation of mean features inherent to vicinities of a large number of strong earthquakes. A strong earthquake vicinity is understood here as a space-time domain where evolution of seismicity is influenced by occurrence of a given strong earthquake. Using the approach presented in (Rodkin, 2008) we have constructed the mean generalized space–time vicinity of a large number of strong earthquakes and examined the mean anomalies inherent to this vicinity.

2. Construction of generalized vicinity of strong earthquake

We have used the Harvard worldwide seismic moment catalog for 1976–2005, and the USGS/NEIC catalog for 1968–2007. In both cases only shallow earthquakes with depth H < 70 km were examined. Two subsets of data can be used, first one includes all earthquakes from the catalog and the second includes stronger earthquakes that are only completely reported. Below we present the results from processing of the Harvard catalog using the first subset of data (all reported events) and the results for the USGS/NEIC catalog using only completely reported events. In the latter case the events with magnitude M ≥ 4.7 were used, a total number of events was 97615. A similar cutoff for the Harvard catalog would reduce the available data too much to get statistically robust results.

Both used data sets were searched for events falling into the space–time domains surrounding the source zones of large (M7+) earthquakes, with due account for the seismic moment in the Harvard catalog and the maximum magnitude for the USGS/NEIC catalog. A generalized vicinity of large earthquake is understood as a set of events falling into the zone of influence of any of these strong earthquakes. The zones of influence were defined as following, see also (Rodkin, 2008) for the details. Spatial dimensions of the zones of influence for earthquakes of different magnitudes were calculated from the approximate relationship (Sobolev & Ponomarev, 2003) between typical source size L and earthquake magnitude M:

$$L\ (\mathrm{km}) = 10^{0.5M - 1.9}. \quad (1)$$

In the examination below the earthquakes located at distances within $7\times L$ from the epicenter of the given strong earthquake were taken into account.

For constructing a time vicinity of strong earthquake we used the conclusion that duration of a failure cycle weakly depends on earthquake magnitude (Smirnov, 2003). Hence the simple epoch superposition method can be used for comparing the time vicinities of earthquakes with close magnitudes. At the figures below all earthquakes located in the area $7\times L$ of the corresponding strong event were taken into account. This choice allows the most complete use of available data. Negative consequences of this choice are a lower statistical significance at the edges of the time interval because of shortage of data there, and a false effect of a systematic growth of a number of earthquakes towards the centre of the used time interval. However these errors can be taken into account, so they do not distort the results.

The generalized vicinity of large earthquake which was constructed contained more than 60000 earthquakes for the Harvard catalog and more than 300000 earthquakes for the USGS/NEIC catalog. Such a big number of events resulted from the fact that one and the same earthquake can belong to the space–time vicinities of different strong earthquakes.

Such an increase in a number of events has considerably enhanced the possibility of statistical examination.
Time and space position of each earthquake falling into the generalized vicinity of large earthquake is characterized by the time shift from the origin time of the corresponding strong earthquake and by the distance from the epicenter of this main event (norm to the source size of this main event). Both catalogs (USGS/NEIC and Harvard) were used for examination of the relative space-time density of earthquakes. The Harvard catalog was used in this paper mostly for the verification of results, which were obtained from examination of the USGS/NEIC catalog.

3. Regularities in rate of fore- and aftershock cascades

The most well known feature of seismic behavior occurring in the vicinities of large earthquakes is the existence of aftershock and foreshock power-law cascades. Figures 1*a* and 1*b* show the foreshock and aftershock sequences in the generalized vicinity of strong earthquake, which were obtained from USGS/NEIC data (similar results were obtained from examination of the Harvard catalog). The earthquakes rate is presented by time density of group of earthquakes consisting of subsequent 50 events taken with step 25 events (rate of events is given in n/day for convenience).
As can be seen in Fig. 1, the evolution of foreshocks and aftershock sequences well correlates with a power law. The Omori law (Utsu et al., 1995; Sobolev, 2003) is known to be a good fit to the aftershock rate:

$$n \sim 1/\ (c + t)^{-p}, \tag{2}$$

where n is the rate of aftershock occurrences, t is the time interval after the main shock occurrence, c – parameter fitting the rate of earthquakes in the closest vicinity of the main shock, and p is the parameter of the Omori law. The Omori law (2) is a good fit for the interval until one hundred days or somewhat later after the main shock occurrence.
The foreshock cascade occurring before the main shock time can be described in a similar manner; in this case t is the time before the main shock origin, and c = 0. The foreshock cascade was found to be quite noticeable in the generalized vicinity 10-20 days before the main shock occurrence (Fig. 1).
Of special interest is the deviation of the aftershock rate from the power law during the first hours after the main shock occurrence. The deficit of earlier aftershocks described by parameter c in (2) is explained sometimes by difficulty in recording all of too numerous aftershocks occurring immediately after a large earthquake. However, this factor is hardly capable of providing a full explanation of the phenomenon (Lennartz et al., 2008; Shebalin, 2006). The deviation from the power law toward lower rates of events during a few first hours of the aftershock sequence can be seen clearly in Fig. 1b; the rate of aftershocks reaches the values obeying the power law only 2–3 hours after the strong earthquake. At that time the mean rate of earthquakes with M ≥ 4.7 occurring in the vicinity of a mean large earthquake (but not in the generalized vicinity of large earthquake) is a little above one event per hour. Such rate can not cause any problem in events recording. Thus, the effect of a lower rate of earlier aftershocks probably has a physical nature. This conclusion is similar with those presented in (Lennartz et al., 2008; Lindman et al., 2010; Shebalin, 2006).

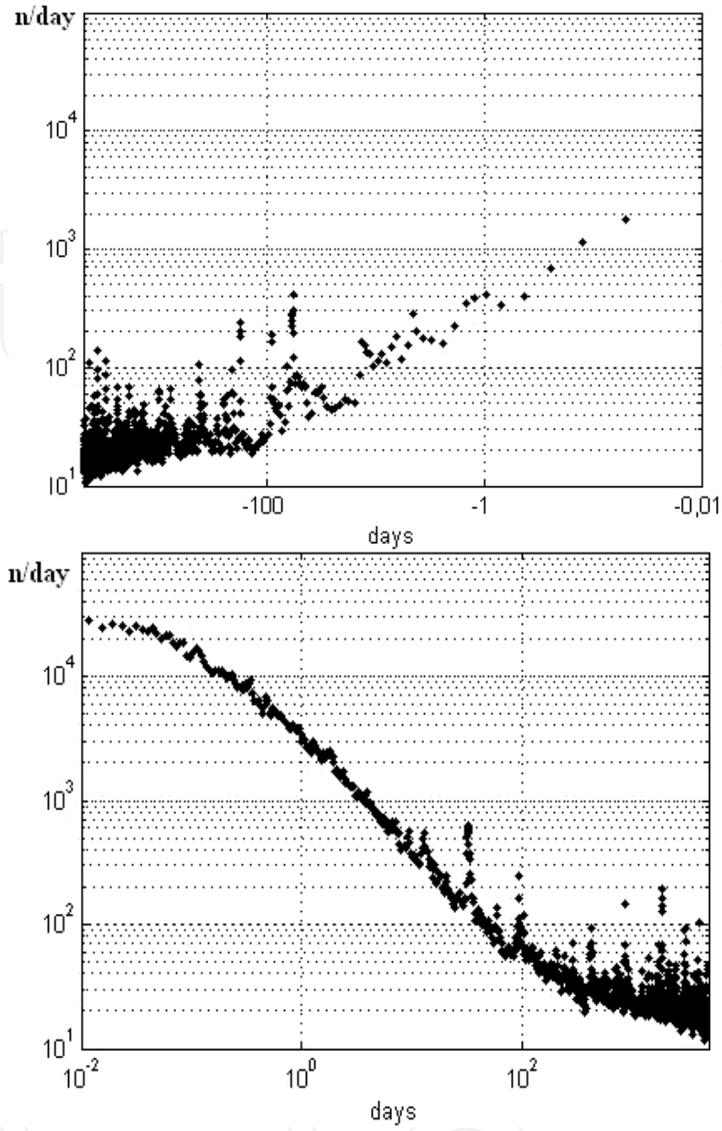

Fig. 1. The fore- (upper panel) and aftershock (lower panel) sequences in the generalized vicinity of strong earthquake, events flow is given in a number of events per day, zero time corresponds to the moment of occurrence of the generalized main shock.

Note that as it can be seen in Fig. 1, the mean duration of the foreshock process is significantly shorter than that of the aftershocks, and the rate of increase for foreshocks toward the moment of main shock occurrence is noticeably slower than the decay of the aftershock rate. From this it follows that the typical maximum rate of foreshock sequence is an order smaller than the maximum rate of aftershock process. This result is intimately related to the problem of predictability of large earthquakes; the prediction problem would have been solved already, if the rate of foreshocks would be equal to the rate of aftershocks. It seems important to note that upon closer examination the seismicity increase in the generalized vicinity of large earthquakes is not confined to the foreshock and aftershock cascades. Essentially weaker but quite noticeable increase above the mean rate level occurs

in the time interval about ±100-300 days around the main shock date. The analysis of the Harvard seismic moment catalog gives similar results; however, these data testify for a broader area of seismicity increase, roughly within ±500 days around the main shock date. This type of long-term pre- and post-shock seismic activity agrees with the suggestion that the final time interval of strong earthquake preparation prolongs a few years.

We now characterize the changes in the seismicity increase as functions of the distance to the main shock epicenter. The distances are compared in units of the magnitude-dependent main shock source dimension L from equation (1). Fig. 2 shows the distance–time diagram of rate of a number of events in the vicinity of the main shock. The horizontal axis indicates the time (in days) from the main shock occurrence time; an analogue of longtime scale is used near the main shock occurrence moment. The vertical axis indicates the distance from the main shock epicenter in units of earthquake source size L. Events' rate is given in logarithmic scale, ln(n), where n is the number of events in a cell of the distance–time diagram.

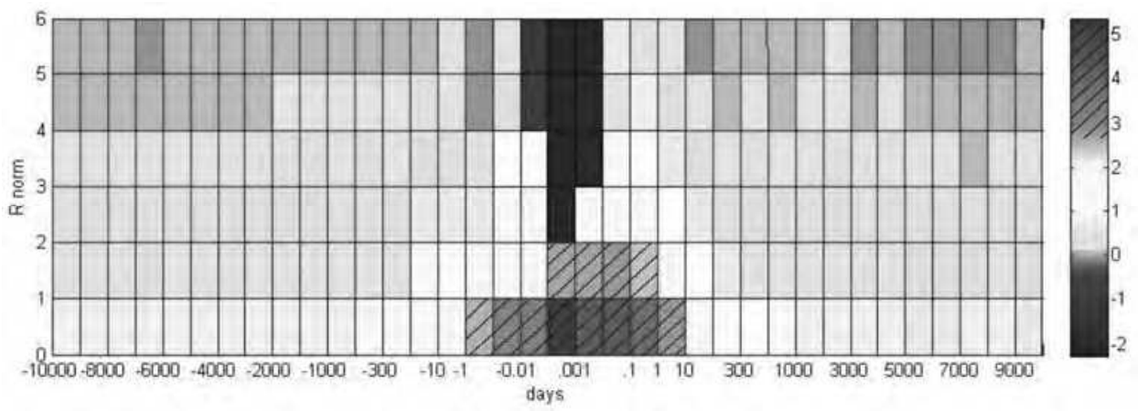

Fig. 2. Spatial-temporal change of number of earthquakes lg (density of events per day) in the generalized vicinity of strong earthquake, distance R_{norm} from the main shock epicenter is given in norm source size units.

As can be seen in Fig. 2, the rate of earthquakes in the vicinity of the main shock begins to increase one-three hundred days before the main shock, and this activity increase accelerates toward the moment of the main shock. The increase in seismic activity occurs at a distance of about three source sizes L from the main shock. This estimate of the radius of influence is in agreement with the size of the areas where predictive functions are usually estimated in earthquake prediction algorithms (Kossobokov, 2005; Shebalin, 2006). Seismic activity outside the zone of 3–4 earthquake source sizes decreases in the close time vicinity of strong earthquake. This feature can result from softening in the source of ongoing strong earthquake. Some other indications of strength decrease in the strong earthquake vicinity are presented in (Rodkin, 2008). In this case one can expect the strain rearrangement from the outer "rigid" region into the inner "soft" zone where the strong earthquake is about to occur. As a result of this rearrangement, the probability of earthquake occurrence in the outer "rigid" zone of the future rupture would become somewhat lower.

The decrease in b-value is known to be used as an indicator of an increase in probability of a strong earthquake occurrence (Shebalin, 2006; Zavyalov, 2006). Catalog USGC/NEIS was

used to examine the change in b-value in the generalized vicinity of strong earthquake (the similar results were obtained from examination of the Harvard catalog). The maximum likelihood method was used for the *b*-values estimation (Utsu, 1965). By this method the *b*-value is calculated from

$$b = lg(e) / (M_{av} - M_c) \tag{3}$$

where M_{av} is the average magnitude for each subset of data and M_c is the lower magnitude limit used in the analysis, here M_c=4.7. Discreteness of magnitude values because of

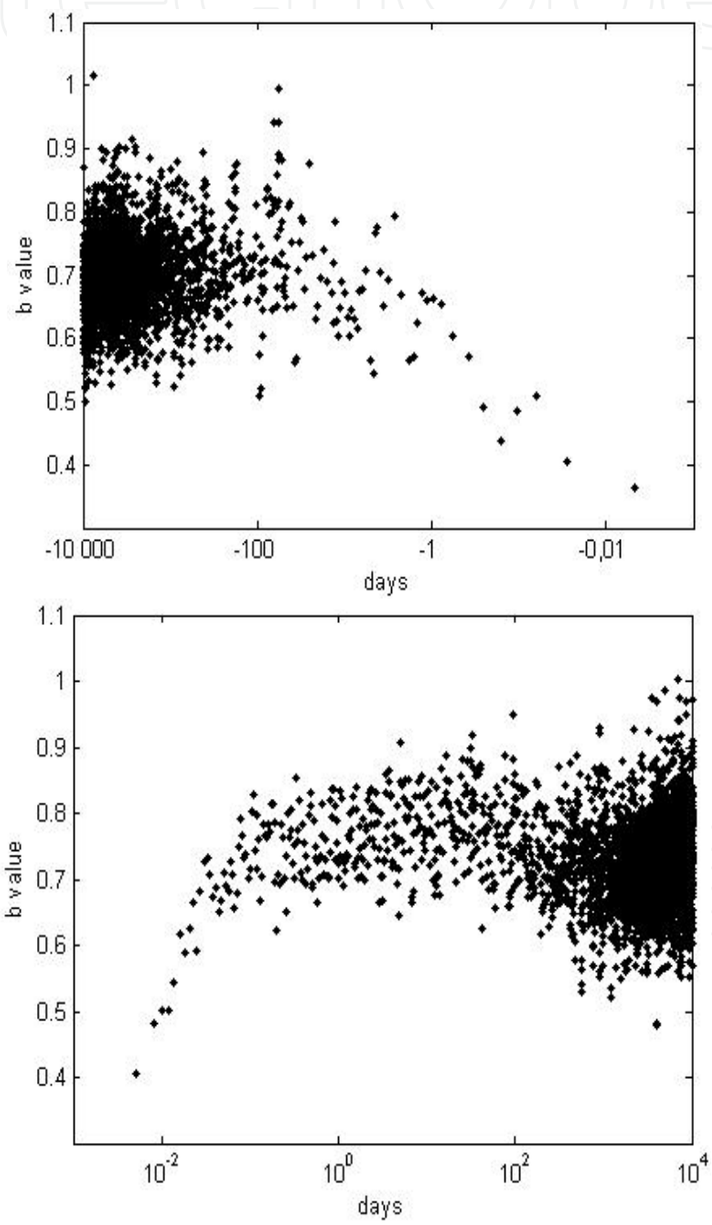

Fig. 3. The change of mean b-values in the generalized vicinity of strong earthquake. The values obtained for 50 events groups are given by dots. Panels as in Fig. 1.

aggregation in 0.1-bins is small, it influences the *b*-values weakly and uniformly; therefore it was not taken into account. The maximum likelihood method (3) gives a suitable *b*-value estimation for a number of events exceeding 50. Having this in mind the groups consisting of 50 subsequent events were used in *b*-value determination. The data points in Fig. 3 reflect the *b*-values obtained for such groups with step 25 events; thus the data points are independent of those next to the adjacent ones.

As it can be seen in Fig. 3, there is an evident tendency of decrease in *b*-values in the time vicinity of the generalized main shock; and this decrease increases strongly with approaching the moment of the main shock. In the foreshock sequence the noticeable decrease begins about one hundred days before the main shock. In the aftershock sequence the sharp increase in *b*-values takes place during the first several days after the main shock. A slow increase in *b*-values takes place in the following 100 days. It is necessary to notice that the *b*-values appear to be increased in comparison with the background value in the time interval 10-100 days after the main shock occurrence. These features agree with a tendency of lowermost *b*-values in the very beginning of the aftershock sequences and with an increase of *b*-value in the further evolution of the aftershock sequences (Rodkin, 2008; Smirnov & Ponomarev, 2004). The similar tendency was found in the examination of acoustic emission data (Smirnov & Ponomarev, 2004). New findings consist in the stronger decrease than it was found before and in rather symmetrical character of this decrease for fore- and aftershock sequences. Note that the amplitude of the *b*-value decrease appears to be proportional to the logarithm of time remaining from the moment of the main shock. Such type of behavior is typical of critical processes.

Note however that the well known and widely used below effect of "seismic quiescence" was not found in the generalized vicinity of strong earthquake. It can be connected with anisotropic character of this type of precursor anomaly in relation to a strong earthquake epicenter that is mentioned in (Zavyalov, 2006). In this case this effect can be eliminated by summarizing data from vicinities of a large number of differently oriented strong earthquakes.

4. Experience in earthquake prediction at the Sakhalin Island and surrounding areas

Region under study includes the Sakhalin Island and the Kuril Islands arc. In a few cases the area of the Japan Islands was also taken into account. This territory belongs to the transitive zone between the Pacific and the Eurasian continent and includes the active island arc characterized by one of the highest levels of seismicity on the Earth. Because of variability in quality of available catalogs the methodology of prognosis is more or less different in every particular case of strong earthquake prognosis, which is described below.

To avoid misunderstanding and controversial interpretations, we follow below the definition of the term "earthquake prediction," which was formulated by the Panel on Earthquake Prediction with the US National Academy of Sciences (Allen et al., 1976):

"An earthquake prediction must specify the expected magnitude range, the geographical area within which it will occur, and the time interval within which it will happen with sufficient precision so that the ultimate success or failure of the prediction can readily be judged. Only by careful recording and analysis of failures as well as successes can the eventual success of the total effort be evaluated and future directions charted. Moreover,

scientists should also assign a confidence level to each prediction." (Predicting earthquakes …, 1976).
In the case when the demands of this definition are not fulfilled the term "earthquake forecasting" is used.
We use such definition instead of another one when the term "prediction" means a deterministic prognosis as it was formulated in (Operational Earthquake Forecasting: State of Knowledge and Guidelines for Utilization. International Commission on Earthquake Forecasting for Civil Protection, http://www.protezionecivile.gov.it/cms/attach/ex_sum_finale_eng1.pdf). We suggest that deterministic prognosis is impossible now and hardly will be possible even in future, thus such use of the term "prediction" seems to be inefficient.

4.1 Case 1 - Diagnostics of a dangerous period before the 1994 Mw 8.3 Shikotan earthquake (the South Kuril region)

4.1.1 Seismic region and data

The region under study in case 1 includes the Kuril Islands zone and the area to the east of Hokkaido Island. In 1992 we have prepared in computing form the earthquake M ≥ 4.0 catalog of the Kuril-Okhotsk region for the period 1962-1990. It was formed on the basis of yearly publications (The earthquakes in USSR…, 1964-1991). During the next years the catalog was updated by the Operative catalog data of the Sakhalin Branch of Geophysical Survey of the RAS. We used this regional catalog for testing the M8 algorithm (Keilis-Borok & Kossobokov, 1986, 1990) which provided a suitable procedure for prediction of large earthquakes.

4.1.2 Methodology

The intermediate-term earthquake prediction technique, named M8 algorithm, is based on an assumption that a number of functions, defined for a particular earthquake sequence, become extremely large in values, within several months prior to a major shock. The functions used are following (Keilis-Borok & Kossobokov, 1986, 1990):
N – cumulative number of main shocks (aftershocks are excluded according to (Keilis-Borok et al., 1980)) describes an increase in seismic activity;
L – describes deviation of N from the long-term trend value;
Z – describes a linear concentration of earthquake sources;
B – describes the bursts of aftershocks.
All functions, except the last one, were calculated twice: for a standard variant of small statistics (10 events or less per year) and for a standard variant of large statistics (20 events or more per year); where the numbers of events change by choice of threshold of magnitude taken into account. Two statistics are used for increasing robustness of results of prognosis. Values of these seven functions were used for adjusting the M8 algorithm, and then for diagnostics of Time of Increased Probability (TIP) for large earthquake (M ≥ 7.5) occurrence within the circular areas with a fixed radius.
Besides the method described above, we used a visualization technique to display space-time distribution of seismicity to detect seismic gaps of the second kind. A gap of the second kind (seismic quiescence) refers here to a portion of a seismic area of low seismic activity with no observed earthquakes with M≥6.0 for a period of several years. This approach follows the concept of K. Mogi (1985).

4.1.3 Results of analysis and precursors phenomena

Seismicity of circular areas with a radius of 427 km with the centers located in the points: 44^0 N, 149^0 E; and 48^0 N, 155^0 E has been examined. These two circles overlap all the territory of

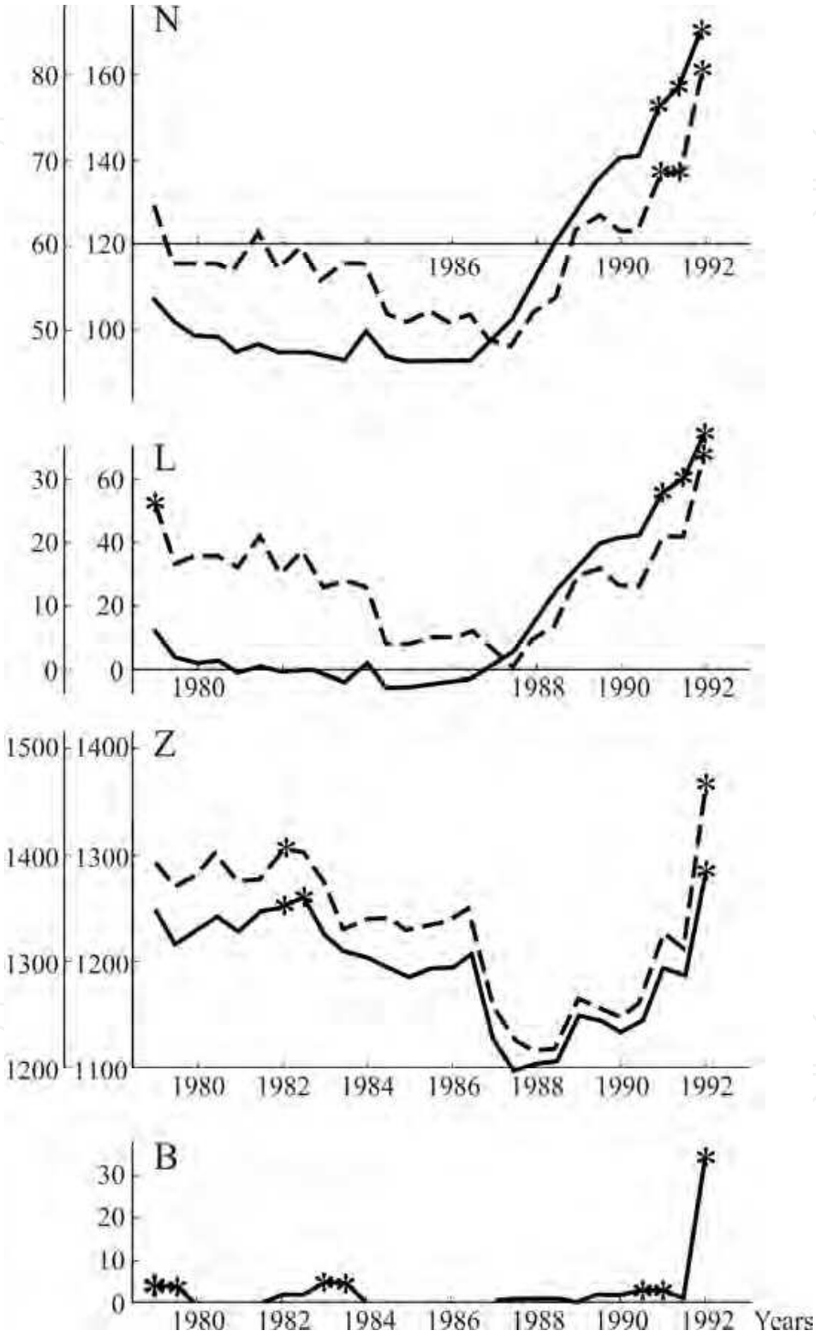

Fig. 4. The behavior in time of seven functions of the M8 algorithm for the Southern Kuril region during the diagnostics period, 1979-1992. The solid lines show the values, calculated for large statistics (20 events or more per year), and the dash lines show the values for small statistics (10 events or less per year). Star symbols mark anomalous values.

the Southern and Northern Kuril Islands. The catalog data have been processed by the M8 algorithm for the time period from 1962 to July 1992, with the functions being calculated for every six months.

Some results of the processing are presented in Fig. 4, which demonstrates the behavior of all seven functions in the first circular area (Southern Kuril Islands) during the diagnostics period (1979-1992). All the functions have become extremely anomalous, large in values to the July of 1992, which means, that the M8 algorithm diagnoses the TIP for a large earthquake occurrence during next 5 years (1993-1997). The alarm should be kept if anomalous values of almost all the functions are kept in the next six months.

The similar results have been derived by the authors of the M8 algorithm on the base of processing of the NEIC/USGS catalog data (Kossobokov et al., 1994, 1996). All needed parameters of the prognosis of the future strong earthquake were indicated, and thus we suggest that in case 1 the term "prediction" is suitable.

For the second circular area (Northern Kuril Islands) anomalous value has been obtained for the B function (bursts of aftershocks) only, and it means, that M8 algorithm diagnoses no TIP for a large earthquake occurrence in this area within the next 5 years.

The above mentioned suggested a high probability of occurrence of large earthquake within the Southern Kuril zone in the nearest years. This suggestion was found to be in an agreement with the space-time distribution of earthquakes with M ≥ 6.0 within the Kuril seismic zone since 1987 (Fig. 5). A large seismic gap of the second kind can be seen within a big area from the southern part of Urup Island to the northern end of Hokkaido Island.

4.1.4 Realization of prediction

The prediction described above was submitted in July of 1992 to the Russian Academy of Sciences and the Ministry of Emergency Situations (REC RAS/EmerCom). It was written in the conclusion that "the Southern Kuril region and the area to the east of Hokkaido Island will remain in a state of high probability of a large (M=7.5-8.5) earthquake occurrence during 5 years, which started since the middle of 1992" (Kossobokov et al., 1994, 1996).

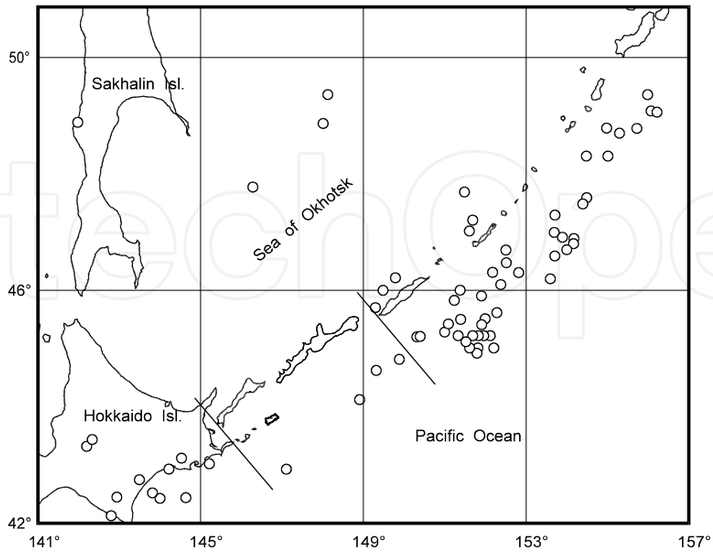

Fig. 5. The distribution of epicenters of earthquakes with M ≥ 6.0 in the Kuril-Hokkaido area for the period from March 1987 to July 1992. The area limited by solid lines is the area seismic gap of the second kind.

A large Mw 8.3 shallow-focus (h ~ 40 km) earthquake has occurred on 04 October 1994 at 13:22 GMT to the east of Shikotan Island (Russia) (Fig. 6). Thus, the intermediate-term prediction of July 1992 was confirmed.

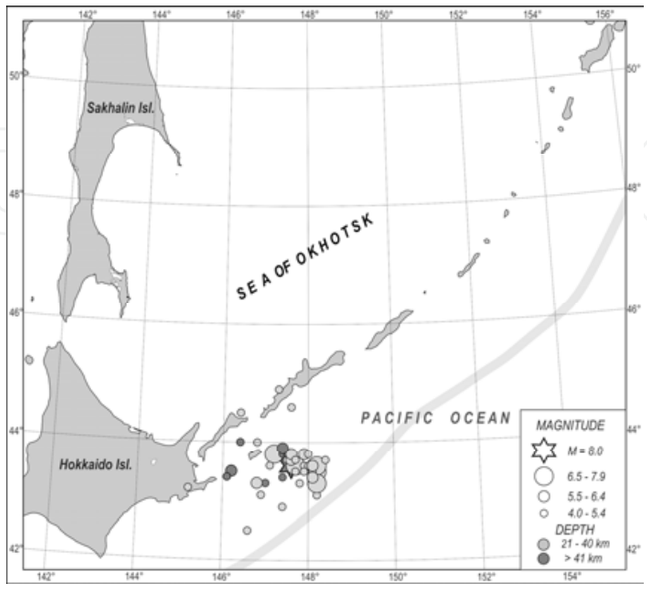

Fig. 6. Epicenters of the 1994, Mw 8.3 Shikotan earthquake and first-day aftershocks of magnitude M ≥ 5.0.

Just before the Mw 8.3 Shikotan earthquake the seismic stations in Kurilsk and at Shikotan Island were closed because of the economic crisis. In this situation we have no data to attempt to perform a short-term prognosis. But using a posteriori data from USGS/NEIC a short-term prognosis of this event was done. We used the method of self-developing processes, which was suggested by Malyshev (Malyshev, 1991; Malyshev et al., 1992). It is described below (case 4) where it was applied in a real time. By the use of this method the one and a half year foreshock sequence of events was analyzed and the date of the strong earthquake occurrence was a posteriori estimated with a few days delay (Fig. 7).

4.1.5 Case 1 summary

Some characteristics of the earthquake flux for the period from 1962 to July 1992 in the Kuril seismic zone have been investigated on the basis of two methods: (1) the intermediate-term earthquake prediction algorithm M8; (2) a visualization of space-time distribution of seismicity. The M8 algorithm diagnosed the Time of Increased Probability for a large earthquake occurrence in the circular area with the radius of 427 km at the point (44^0 N, 149^0 E) during the period 1993-1997. By means of the second method the seismic gap of the second kind was detected within a big area from the southern part of Urup Island to the northern end of Hokkaido Island. The quiescence began in March 1987. A catastrophic shallow-focus (h ~ 40 km) Mw 8.3 earthquake has occurred on 04 October 1994 at 13:22 GMT to the east of Shikotan Island (Russia).

A posteriori short-term prognosis by the method of self-developing processes data was performed using USGS/NEIC data. The date of the strong earthquake occurrence was a posteriori estimated with a few days delay (Fig. 7).

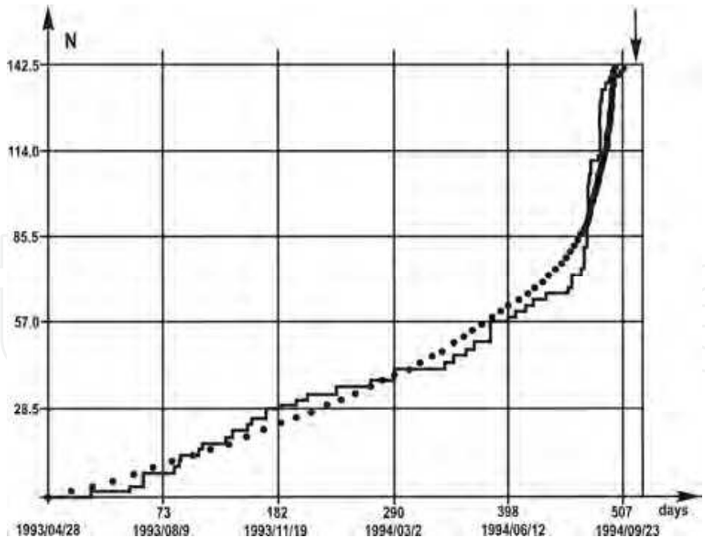

Fig. 7. The cumulative number of earthquakes observed by USGS/NEIC in the Southern Kuril Islands area as a function of time through April 1993–November 1994.

The stair-case curve is empirical data, and the smooth curve simulates the data according to the method of self-developing processes. The vertical line is the asymptote corresponding to the prognostic event date three days after the earthquake occurrence (the arrow).

4.2 Case 2 - Partly retrospective forecasting of the May 27, 1995 Mw 7.1 Neftegorsk earthquake, North-Eastern part of Sakhalin Island, Russia

4.2.1 Seismic region and data

Seismicity of the northern part of the Sakhalin region (north of latitude 50^0 N) was the object of this investigation. It had a moderate level of seismicity in comparison with seismic activity of the Kuril Islands. Destructive earthquakes like the 1995 Mw 7.1 Neftegorsk earthquake are rare events here. Paleoseismological reconstruction within the Upper Piltun fault, which was reactivated during the Neftegorsk earthquake, showed that recurrence of such earthquake is about one event per several hundred years (Shimamoto et al., 1996). Seismicity patterns were analyzed on the basis of the regional catalog of shallow-focus $M \geq 3.0$ earthquakes, issued by ESSN (The earthquakes in USSR…, 1964-1991).

4.2.2 Methodology

In this case same methods as in the case of the Shikotan earthquake were used. A magnitude for identification of a seismic quiescence area for the Sakhalin region was taken M = 3.0.

4.2.3 Results of analysis and precursors phenomena

The second kind seismic gap area taking place along the eastern coast of the Northern Sakhalin has indicated the approximate location of a possible future large earthquake (Fig. 8) (Kim, 1989). The gap of the second kind was recognized in 1989, i.e. 6 years before the Neftegorsk earthquake, it was outlined in the area of 200 by 60 km including the shelf and coastal areas from the southern part of the Shmidt Peninsula to the Gulf of Chaivo. There were no earthquakes with $M \geq 3$ in this area since 1984.

We have confirmed the existence of the quiescence zone in (Saprygin et al., 1993). In this paper we advised to reinforce the Northern Sakhalin network of seismic monitoring. However, in this very time because of the economic problems in this country four seismic stations from six, which controlled this region, were closed down. A large number of objects of industrial and civilian purposes were built with the reference seismicity of 6-7 of the *MSK*-64 intensity scale. Thus, there was a deficit of seismic-resistant buildings and structures. That became evident when the May 27, 1995 Neftegorsk earthquake has occurred. The observed ground shaking intensity was 8-9 (MSK-64 scale) in Neftegorsk, and 1841 inhabitants were killed (A memory …, 2000; Streltsov, 2005).

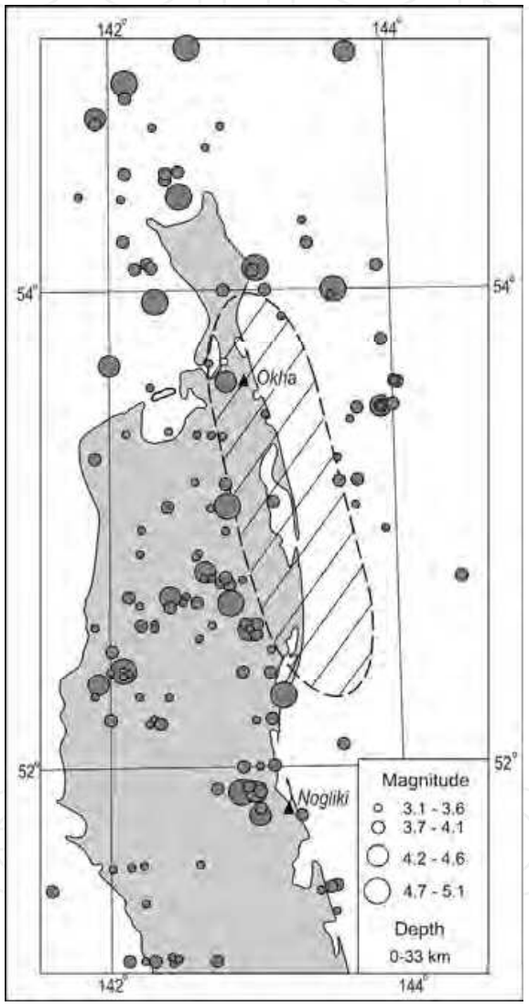

Fig. 8. A seismic quiescence zone (hatched area) in the northern region of Sakhalin Island recognized on the basis of absence the magnitude M ≥ 3.0 events since July 1984 (Kim, 1989). The map shows a state of seismicity in April 1988.

We have investigated the intermediate-term precursors of the Neftegorsk earthquake by means of the M8 algorithm (Keilis-Borok & Kossobokov, 1986, 1990; Tikhonov, 2000). It was applied for the retrospective diagnostics of TIP for this earthquake. We used the declustered

regional catalog (Keilis-Borok et al., 1980). The M8 algorithm was adjusted to the earthquake catalog for the period 1964 – 1978. A dangerous period was found after 1979 (Fig. 9).
In this case data processing was performed under a strong shortage of data (only 4-5 events per year). Dr. Kossobokov analyzed two cases in the similar poor data conditions for the use of the M8 algorithm - deep earthquakes of the Vrancha region (Kossobokov, 1986) and seismicity in Greece (Latoussakis & Kossobokov, 1990). In the first case small and "large" statistics was equal to 2 and 4 events per year but in the second case it was equal to 5 and 10 events per year. However, even under such unfavorable conditions the M8 algorithm has demonstrated an ability to recognize the danger.
In our case only one dangerous period was revealed a posteriori since 1991 when six functions became anomalous (B function was undefined because of poor statistics of small earthquakes). The alarm period was interrupted by the May 27, 1995 Mw 7.1 Neftegorsk earthquake (Fig. 10).

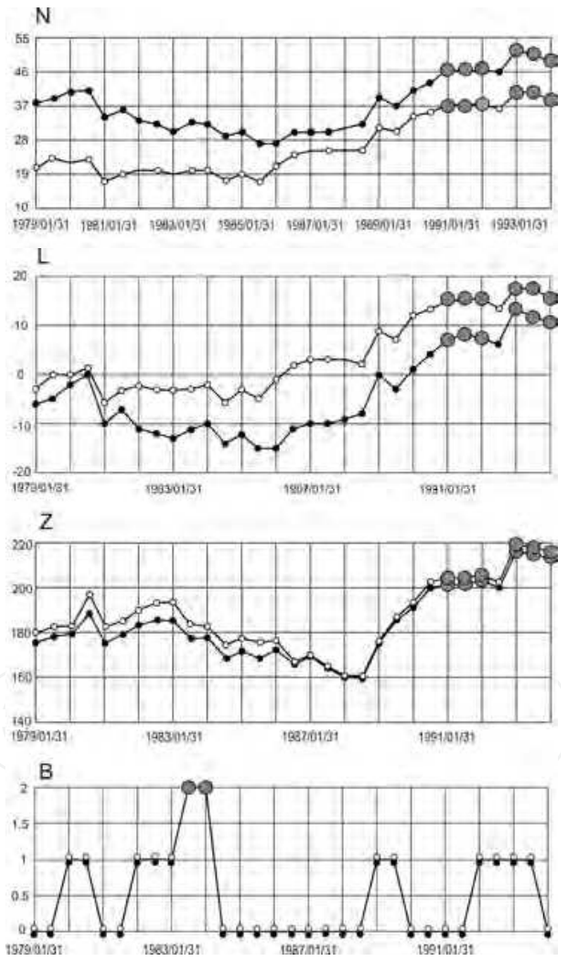

Fig. 9. The behavior in time of seven functions of the algorithm M8 for the northern region of Sakhalin Island during the diagnostics period (1979-1993) before the May 27, 1995 Mw 7.1 Neftegorsk earthquake (Tikhonov, 2000). The white circles show the values, calculated for "large" statistics (5 events or more per year), and the black circles show the values for small statistics (4 events or less per year). Large black circles mark anomalous values.

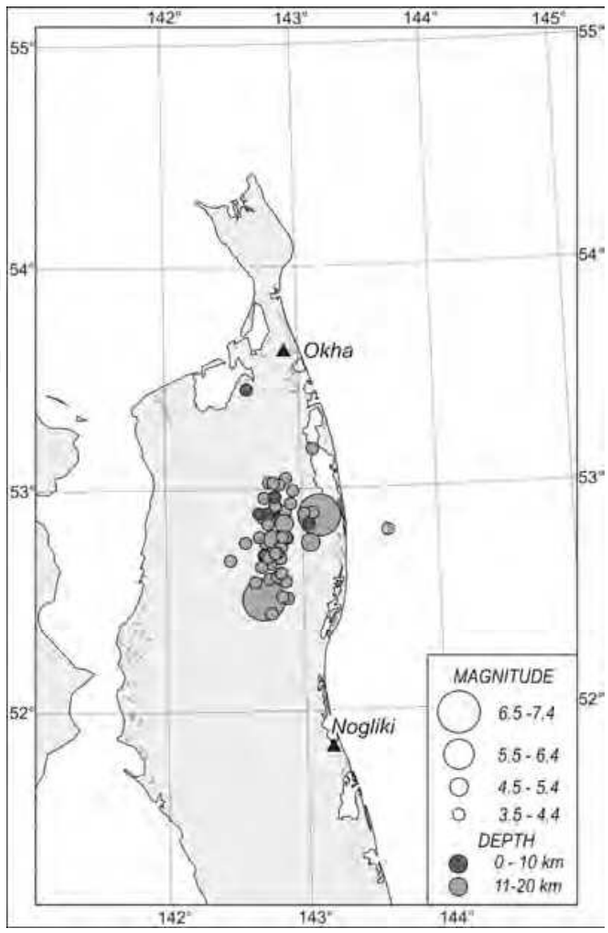

Fig. 10. Epicenters of the May 27, 1995 Mw 7.1 Neftegorsk earthquake and first-day aftershocks of magnitude M ≥ 3.5.

4.3 Case 3 - Incomplete forecasting of the Tokachi-oki Mw 8.3 earthquake (Hokkaido Island, Japan)

The M8 algorithm has failed in prognosis of the Tokachi-oki Mw 8.3 earthquake (http://mitp.ru/predictions/html, this site is of access for experts only since 2000 year). Despite of the failure of the M8 algorithm, the described below ZMAP-technique performed by one of the authors was successful (Tikhonov, 2003; 2005).

4.3.1 Seismic region and data

In this case the territory of the Japanese Islands including the adjacent shelf areas (Fig. 11) was examined. The Japan Meteorological Agency earthquake catalog from January 1974 until July 2002 was used. Earthquakes with M ≥ 3.8, H ≤ 100 km were found to be completely recorded, and these events were taken into account (Fig. 11). This data set is quite homogeneous throughout the whole region of Japan. It permits to apply the ZMAP-technique (Wiemer & Wyss, 1994) for examination. This method could not be applied in the cases 1 and 2 because of a shortage of data and difference in data availability for the Northern and Southern areas of the Sakhalin Island.

4.3.2 Methodology

The ZMAP method (Wiemer & Wyss, 1994) was developed to reveal a change in rate of seismicity as a function of space and time. The authors have used a rectangular grid with a spacing of 2 km for the total studied area about 100 by 100 km. For each grid point N_i nearest epicenters are selected and the maximum distance of an earthquake from the i-th grid point $r(N_i)$ was calculated. Thus the defined $r(N_i)$ is a function of space proportional to the local density of earthquakes. The significance of change in seismicity rate for each grid point is evaluated using the standard z test (Habermann, 1981, 1982)

$$z(t) = (R_{\text{all}} - R_{wl}) \,/\, (\sigma^2_{\text{all}} \,/\, n_{\text{all}} + \sigma^2_{wl} \,/\, n_{wl})^{1/2}, \tag{4}$$

where R_{all} и R_{wl} are the mean rates of seismic process in all observation period (from t_o to t_e) and in sliding window wl, respectively. n indicates the number of samples, σ is the standard deviation.

To visualize the changes in the rate of seismicity the authors plotted z(t) values on a map. Moment t moves through the whole period of the catalog from t_o to t_e. To identify the strongest rate changes between two intervals (from t_o to t and from t to t_e) they have used the $AS(t)$ function (*Habermann, 1983, 1987, 1991*). This function gives the most probable moment of seismic quiescence occurrence:

$$AS(t) = (R_1 - R_2) \,/\, (\sigma^2_1 \,/\, n_1 + \sigma^2_2 \,/\, n_2)^{1/2}, \tag{5}$$

where R_1 , R_2 are the mean rates of seismic process in two periods (from t_o to t and from t to t_e), n_1 and n_2 are the numbers of samples in these periods, σ_1, σ_2 are the standard deviations in these periods.

In the process of application of the ZMAP-technique the following tasks were executed for detection of seismic quiescence periods in the Japan region (Tikhonov, 2003, 2005):

- A modification of the ZMAP-method for application to a large territory in a real time scale has been executed. After the modification the task was implemented using the standard deviate z test (Habermann, 1981, 1982) in two steps: (1) Detection of seismic quiescence in a studied region using a coarse rectangular grid with a moderate number of nodes (with a spacing of 0.25^0); (2) Covering the cells where seismic quiescence was detected by a detailed grid (with a spacing of 0.1^0) and calculation of a configuration of anomalous area with a given value of seismicity rate decrease.
- An adjusting of the modified ZMAP-technique to the JMA earthquake catalog for the detection of possible seismic quiescence periods before the strong shallow earthquakes with $M \geq 6.8$, $H \leq 100$ km.
- An investigation of the precursor seismic quiescence since July 2001 within the studied area.

4.3.3 Results of analysis and precursors phenomena

In order to effectuate the first step of methodology we divided the studied territory into grids spacing 0.25^0 in latitude and longitude (Fig. 11). An adjustment of a modified method was performed to the declustered earthquake catalog for the period 1975 – 1988. The values of $z(t)$ function were identified as anomalous if they exceeded a proper threshold calculated for the adjusting time span. Thresholds U_i for detection of quiescence in separate nodes was defined in the following way:

$$U_i\,(coef) = \mu_i + coef\ \sigma_i\,, \tag{6}$$

where μ_i , σ_i are the average and the root mean square values of function $z(t)$ in node i for the learning time, respectively; *coef* is empirical constant. The value of $z(t)$ were identified as anomalous if $z(t) \geq U_i$ *(coef)*. The constant *coef* was taken equal to 4. Thresholds for nodes were selected to minimize a probability of omission of a real seismic quiescence prior the strong earthquakes with M ≥ 6.8.

Detection of the areas with anomalous values of $z(t)$ function has been fulfilled for the declustered catalog data since 1989. Thus, there were facilities for detection of seismic quiescence periods occurring prior a series of large seismic events, which occurred in 1992 – 2002. As a result, we obtained a set of maps of the Japan region showing the location of such areas at different moments of time. Dynamics of the appearance and evolution of the anomalous areas was compared visually with dynamics of the occurrence of the strong earthquakes (M ≥ 6.8, H ≤ 100 km). It was established that correlation between the most outstanding anomalies and the strong earthquakes was suitable in space and time. In general the maximum size of anomaly is observed about 0.5 – 1.5 yr before the corresponding strong shock. The results of processing of the catalog since 1989 were the following: in 7 cases the occurrence of the strong seismic events was forestalled by seismic quiescence near its epicenters. In general the epicenter is located near the border of the corresponding anomalous zone. In two cases there was no quiescence before the strong earthquakes, and in two cases anomalous areas were observed before swarms of moderate size earthquakes (M = 6.2 – 6.6).

Obviously, the recent seismic quiescence zone revealed in the northern part of Japan had attracted an interest (Fig. 12). The term "recent" dates here back to the time of investigation (the middle of 2002). As a result of the second step of the procedure (with a detailed spacing of 0.1^0 grid size) the most outstanding recent anomaly of 75 km size was located near the Cape Erimo (Hokkaido Isl.) (Fig. 13). It was characterized by a seismicity rate decrease of 75% starting from January 1998. Inside this anomalous area there was a circle with R=25 km with no earthquake occurrence with M≥ 3.8, H ≤ 100.

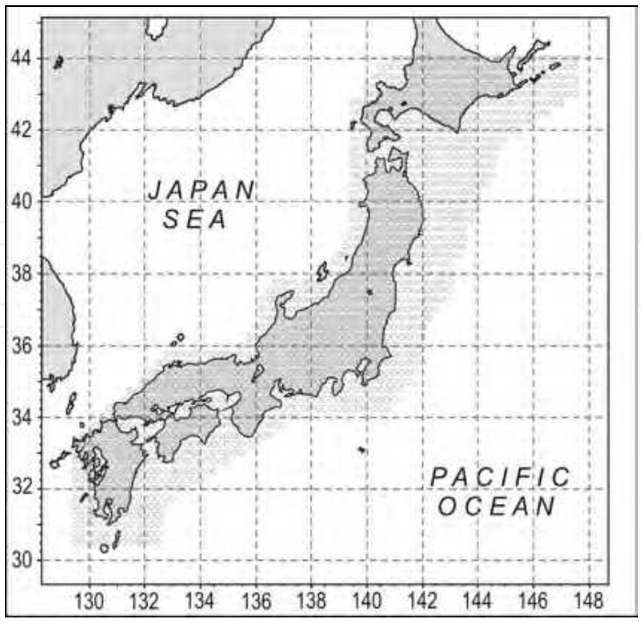

Fig. 11. Map displaying the grid with spacing of 0.25^0 used for detection of seismic quiescence. This grid contains 1354 nodes.

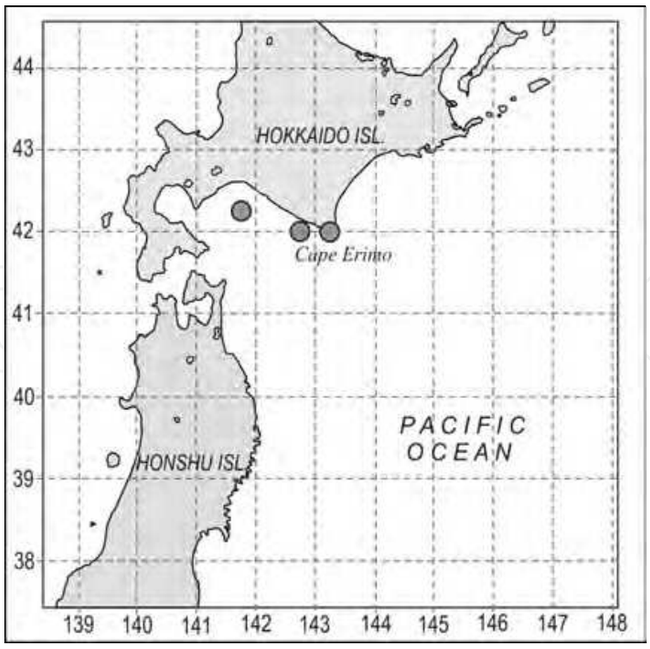

Fig. 12. The location of the seismic quiescence in the northern part of Japan as on June 1, 2002. Gray circles denote the anomalous nodes. The anomaly of seismic quiescence started in January 1998.

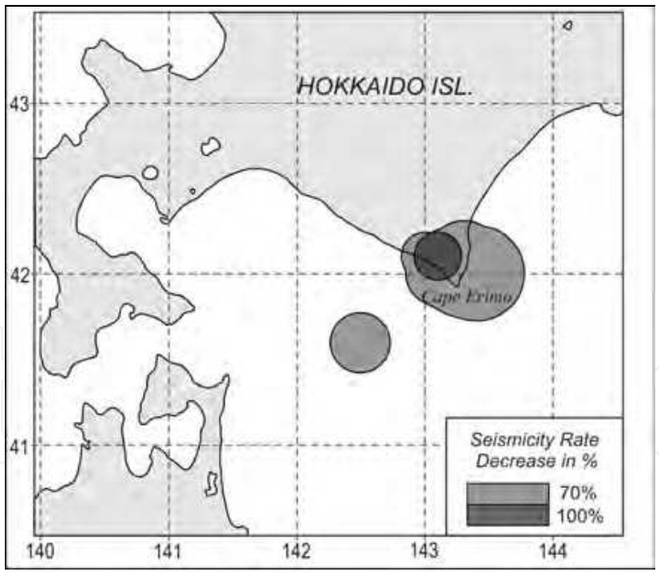

Fig. 13. Map of the seismicity rate decrease calculated for the grid with spacing of 0.1^0 at the middle of 2002. The seismic quiescence anomaly within the Cape Erimo started in January 1998.

4.3.4 The realization of forecasting

The Tokach-oki earthquake forecasting was presented during the XXIII General Assembly of IUGG, which was held in Sapporo (June 30 – July 11, 2003) (Tikhonov, 2003). Besides, these

results were published in (Tikhonov, 2005). The manuscript of the paper was received by the Journal of Volcanology and Seismology on 6 August 2003, i.e. before the occurrence of the Tokachi-oki earthquake. The Tokachi-oki earthquake Mw 8.3 occurred on September 26, at 4 h 50 min JST time near the southern coast of Hokkaido close to the seismic quiescence zone (Fig. 14).

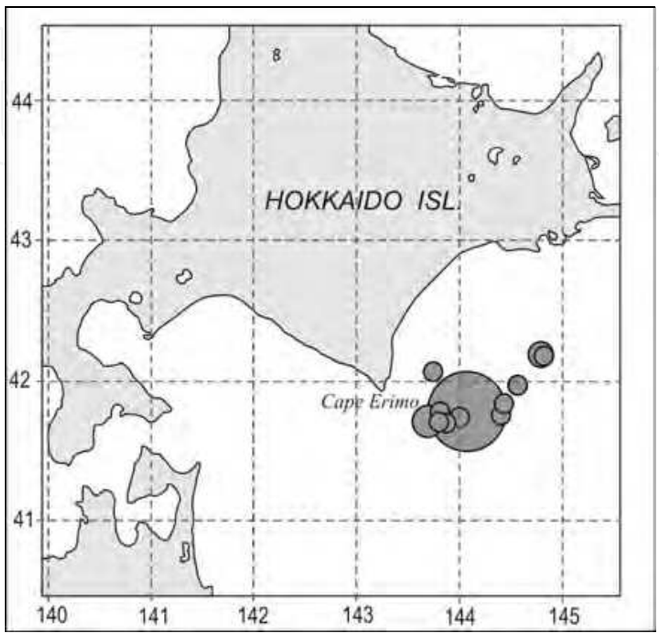

Fig. 14. Map of the 26 September, Mw 8.3 Tokachi-oki earthquake epicenter (large circle) and its first-day aftershocks of magnitude M≥5.0 (small circles).

4.3.5 Case 3 summary

The modified ZMAP-method has been applied to detect precursory seismic quiescence zones in the Japan region. The anomalies revealed for the period 1989 – 2000 correlate in space and time with the strong event occurrences. The greatest size of anomalous area took place typically about 0.5 – 1.5 yr before the corresponding strong shock.

The anomalous decrease of shallow seismicity (M ≥ 3.8) was detected in the southern part of Hokkaido islands at the middle of 2002. In result of the second stage of the procedure the anomaly of 75 km size was determined. It was characterized by a seismicity rate decrease of 75% from January 1998. Moreover, inside this zone there was a circle of 25 km radius with 100% decrease of the rate. The Tokachi-oki earthquake Mw 8.3 has occurred on September 26, at 4 h 50 min JST time close to the seismic quiescence zone (Fig. 14).

4.4 Case 4 - A successful prediction of the 2 August, 2007 Nevelsk earthquake (Mw 6.2) in Southern Sakhalin Island

4.4.1 Seismic region and data

The object of this investigation was the southern part of the Sakhalin Island (south of latitude 48°N). The basic feature of the Earth's crust in this region is characterized by close

arrangement of three major fault systems marked by recent seismic activity. These are the Rebun–Moneron, the Western, and the Central Sakhalin fault zones (Fig. 15).

We used two data sets in this study: (1) the catalog of shallow earthquakes for 1992–2002 from the IRIS-2 system, installed at the "Yuzhno-Sakhalinsk" seismic station in 1992 (Kraeva, 2003); (2) the catalog of network of digital "Datamark" and "DAT" autonomous seismic stations, operating since 2001. The first catalog provides a record of all M > 2.6 seismic events within epicenter distances up to 70 km from the station. The second catalog is more detailed and provides analysis of seismicity patterns in the whole southern part of Sakhalin Island.

4.4.2 Methodology

This prediction was based on the detection of seismic gaps of the first and second kind. Let us describe these terms for the examined situation of the moderate seismic activity of the Sakhalin Island in detail. A gap of the first kind refers to a portion of a seismic area that has been in a state of relative rest for a long time (100 years and more), i.e., there have been no earthquakes with magnitude M ≥ 6.0 during this period. A gap of the second kind (seismic quiescence) refers to a portion of a seismic area of low seismic activity with no earthquakes with M ≥ 3.0 observed for a period of several years. Note that in the case 1 the second kind gap was examined for the magnitude threshold M = 6.0 because of the higher seismic level of the Kuril Islands.

We have used also the method of self-developing processes suggested by Malyshev (Malyshev, 1991; Malyshev et al., 1992). It was found that behavior of empirical earthquake sequences before and after large seismic events is satisfactory described by solutions of a nonlinear differential equation of the second order:

$$\frac{d^2x}{dt^2} = k\left|\left(\frac{dx}{dt}\right)^2 - V_0^2\right|^{\gamma}, \tag{7}$$

where x is a parameter of process (for example, a cumulative sum of a number of shocks – N parameter), $V_0 = \left(dx/dt\right)_0$ is a rate of seismic process in stationary state, k and γ are empirical constants. Particular solution of the equation in case of $2\gamma > 1$ has a vertical asymptote. The time position of this asymptote is shown to be close to the origin time of the ongoing strong earthquake.

4.4.3 Precursors phenomena and characteristics of prediction

Apparently, each of three above mentioned fault zones has the potential to originate major earthquakes Ms 7.0–7.5. However, evidence is currently limited to the Rebun–Moneron (the 1971 Moneron earthquake, Ms 7.5) and the Central Sakhalin (paleoseismological data) fault zones. The Western Sakhalin fault zone showed no magnitude M > 5.0 events in its southern part during the whole history of instrumental observations up to 2006 (Fig. 15). However in its northern part (latitude>48°N) it has originated large earthquakes in 1907 (Alexandrovsk–Sakhalinsk, Ms 6.5), 1924 (Lesogorsk–Uglegorsk, Ms 6.9), and 2000 (Uglegorsk, Ms 7.2) (Fig. 16). Besides these three major fault zones in the studied area there are a number of small fault zones of lower seismic potential.

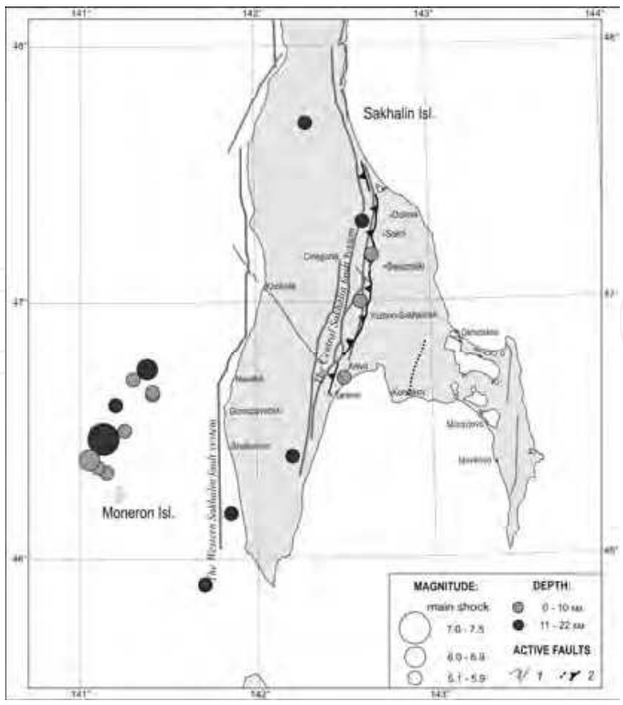

Fig. 15. Map of crust earthquake M > 5.0 epicenters of southern Sakhalin, 1906–2005, and the main fault zones.
Notes: The active faults are plotted according to M.I. Streltsov of IMG&G FEB RAS, Yuzhno-Sakhalinsk (1) and A.I. Kozhurin, of GIN AS, Moscow (2).

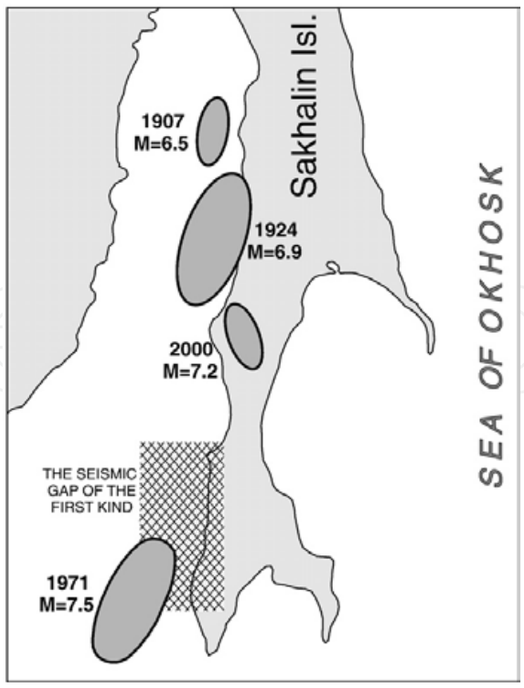

Fig. 16. Sources of large earthquakes at the western coast of Sakhalin Island (grey ovals) and the approximate location of the seismic gap of the first kind (hatched rectangle).

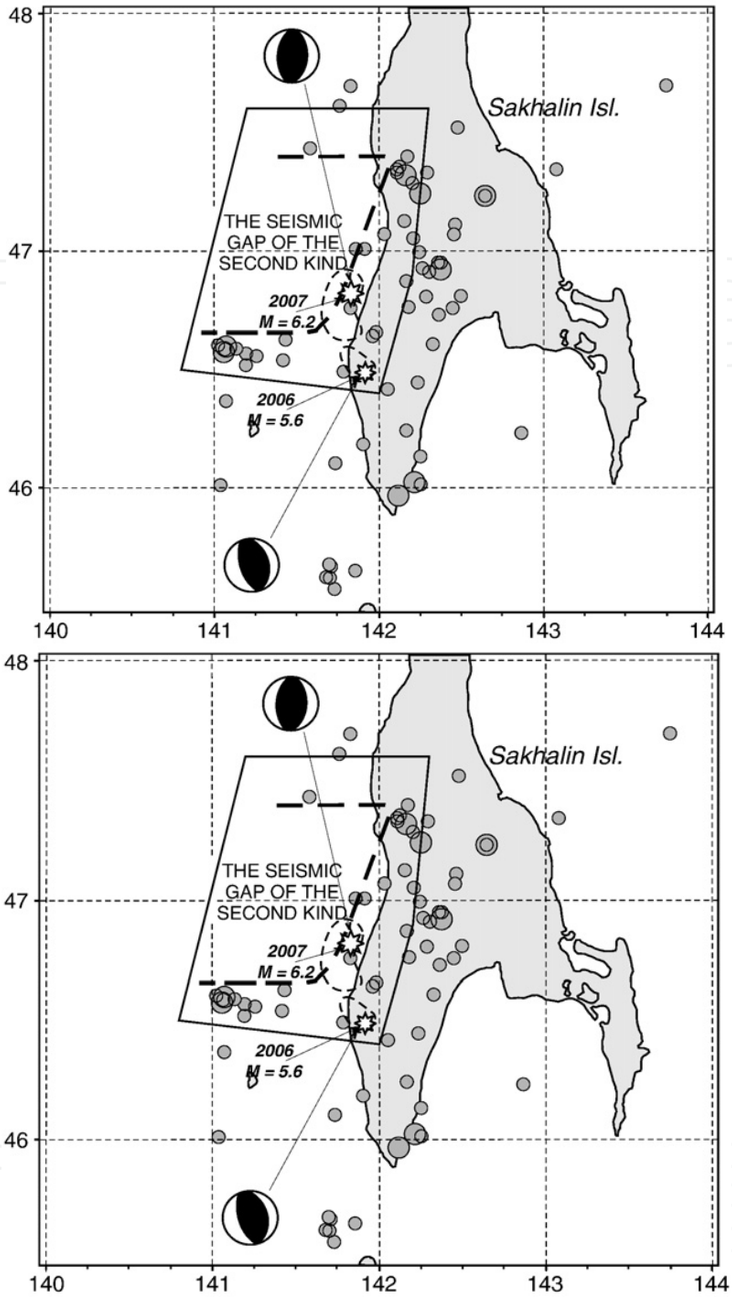

Fig. 17. Map of crust earthquake M≥3.0 epicenters, 1993–2005, recorded by the "Datamark" network of stations and the "IRIS-2" system, installed at the "Yuzhno–Sakhalinsk" seismic station.
Note: the area of the seismic gap of the second kind is outlined with the bold dash line, while the source zones of the 17 August 2006, Mw 5.6 Gornozavodsk and the 2 August 2007, Mw 6.2 Nevelsk earthquakes, with a thin dash line; asterisks indicate the epicenters of main shocks; focal mechanisms are given based on data from [http://www.globalcmt.org]. The area limited by the polygon is the geographical area within which a large earthquake M=6.6±0.6 may occur.

An earlier publication (Tikhonov, 1997) recognized an incipient of the second kind gap (seismic quiescence) within one of the gaps of the first kind, situated on the western coast of southern Sakhalin. In December 2005 our analysis of the southern Sakhalin network data permitted to made it possible to: (1) outline rather precisely the area of a seismic gap of the second kind, where shallow earthquakes with magnitudeM ≥ 3.0 did not occur from at least the middle of 2003 (Fig. 17); and (2) observe the appreciable revival of seismic activity that eventually encircled this area by 2003 (Fig. 18).

Furthermore, the rise of activity around the seismic quiescence zone, and the area south of it, has accelerated (Fig. 18) with culminations linked to the 30 May 2004 Kostroma, Ms=4.8 earthquake in the Western Sakhalin fault zone and the 18 December 2004 Moneron, Ms=4.7 earthquake in the epicenter area of the major 1971 Moneron earthquake. This happened while the seismic sequence of the abovementioned 2001 Takoye earthquake swarm in the Central Sakhalin fault zone was still ongoing.

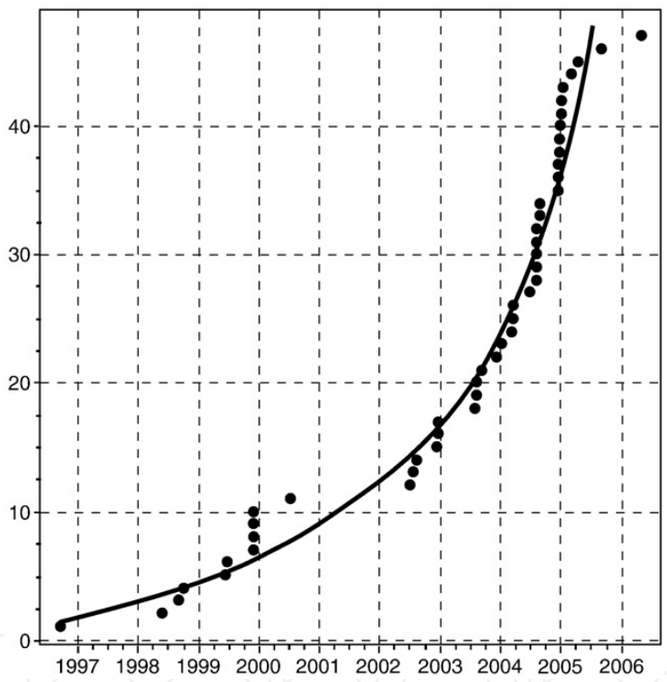

Fig. 18. The cumulative number of shallow earthquakes (depth above 30 km) of magnitude 3 or more inside 45.5–46.75°N and 140.8–142.2°E (i.e., next to the southern area of the identified seismic gap of the second kind) as a function of time in September 1996–May 2006.
Note: the smooth line models the inverse power law acceleration of the empirical data according to the method suggested by Malyshev et al. (1992). The line has the asymptote at 26 August 2007.

At the time, Dr. Tikhonov, in collaboration with Ch.U. Kim, A.I. Ivashchenko and L.N. Poplavskaya (Institute of Marine Geology and Geophysics, Yuzhno–Sakhalinsk) issued the long-term prediction of major earthquake near the western coast of southern Sakhalin (Tikhonov, 2006). This strong earthquake prediction summarized in Table 1 was made by taking into account 1) the seismic gap of the first kind in the Western Sakhalin system of faults, where large earthquakes were absent for at least 100 years (Fig. 16); 2) the seismic gap

of the second kind in the area of 90 by 60 km where seismic quiescence was confirmed by accurate data from "Datamark" digital network (Fig. 17); and 3) the accelerated sequence of earthquakes in the area adjacent to it (Fig. 18). The prediction was the following:

- The location of the incipient hypocenter is most likely to occur at shallow depths within 0–30 km inside the polygon (Fig. 17): (47.6° N; 141.2° E); (46.5° N; 140.8° E); (46.4° N; 142.0° E); (46.9° N; 142.2° E); (47.6° N; 142.3° E).
- The magnitude Ms of the incipient event was estimated in two different ways. The first is the formula by K. Tanaka (1980) lg R=0.33 M−0.07, which relates the linear size of the gap of the second kind, R, to the magnitude of expected earthquake, M. It was used first to determine the expected magnitude M=6.1.
- The second estimate was obtained from the two empirical relations: (1) lg L=(0.5±0.01) M−(1.77±0.07) (Tarakanov, 1995); and (2) L ≈ 1/3 R, where L is the linear size of the aftershock zone (Shebalin, 1961). Substituting an expression (2) in the formula (1), we obtain:

$$\lg R=(0.5\pm0.01)\,M-(1.77\pm0.07)+\lg 3. \quad (8)$$

  This gives M=6.6.
- Of the two estimates, the second appears to be preferable because it takes into account the worst earthquake scenario as well as some uncertainty in estimates. Therefore, Ms=6.6±0.6 was selected as a final magnitude estimate of the expected large earthquake.
- The duration of alarm was determined to be about 7.5 years. This was based on an average time-span of approximately 10 years, observed for seismic quiescence zones that occurred before large earthquakes off the western coast of Japan and Sakhalin, while accounting for no less than 2.5 years of a given quiescence zone's initiation.
- The likelihood of an earthquake occurrence was estimated at 75%, based on the recurrence rate of the large (M ≥ 6.5) earthquakes in the south of Sakhalin (Oskorbin & Bobkov, 1997) and the lifespan of a given quiescence zone.
- The expected intensity of ground shaking (in the MSK-64 scale) was calculated for the three epicenter locations inside the seismic gap of the second kind and the magnitude close to the maximal expected. Fig. 19 displays the results obtained with the epicenter in the middle of the quiescence zone.

The beginning and end of alarm	Magnitude and depth of earthquake	Position of earthquake epicenter	Probability of earthquake occurrence	Maximal macroseismic effect (MSK-64 scale)
January, 2006– July, 2013	M_S = 6.0 – 7.2 h = 0 – 30 km	See the text and Fig. 17	≥75%	9.0 (in epicenter) 8.0 (at the coast)

Table 1. Characteristics of anticipated earthquake (Tikhonov, 2006, page 179).

The prediction described was submitted in January 2006 to the Russian Expert Council for Earthquake Prediction, Seismic Hazard and Risk of the Russian Academy of Sciences and the Ministry of Emergency Situations (REC RAS/EmerCom). As a result of the discussion at the REC Meeting, the prediction was approved as being scientifically motivated. It was then reported to EmerCom headquarters, which had run urgent command-staff exercises in August 2006, referred to as "Mitigating the consequences of destructive earthquake and

tsunami in Sakhalin–Kuril region." The scientific motivations of the prediction have been published (Tikhonov, 2006).

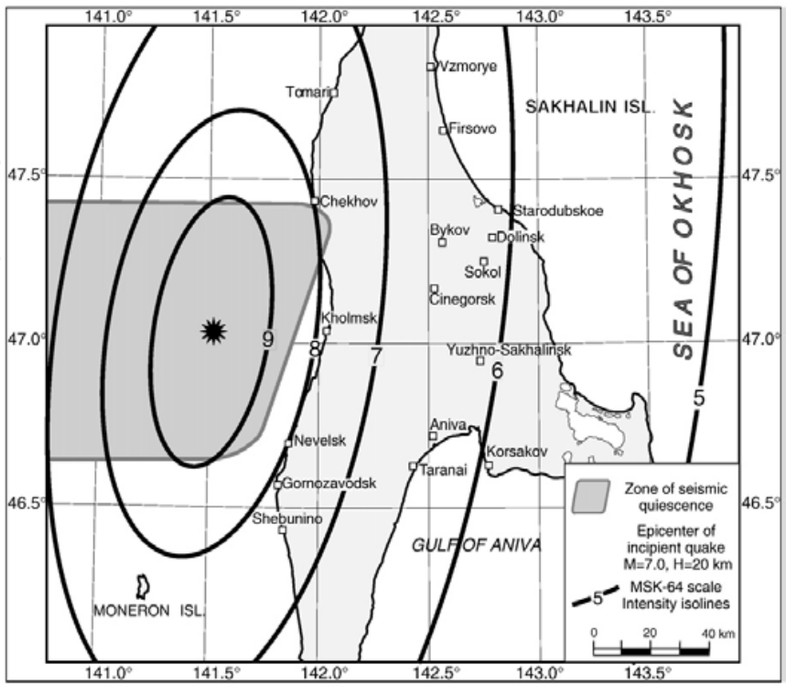

Fig. 19. An expected ground shaking intensity (MSK-64 scale) for the model occurrence of an earthquake of Ms 7.0 at a depth of 20 km in the central part of the seismic quiescence zone (computations by L.N. Poplavskaya of IMG&G FEB RAS made in December 2005).

4.4.4 The realization of the prediction

On 17 August 2006, a magnitude Mw 5.6 earthquake hit the Gornozavodsk settlement in the area of prediction (Levin et al., 2007). Upon analyzing the main shock and its aftershocks, a conclusion of the precursory character of this sequence was drawn. Specifically, it was concluded that the preparation of a large earthquake in the seismic quiescence zone had switched from a long-term to a short-term phase.

This was briefly formulated in the cover letter of an interim report to REC RAS/EmerCom, as follows: "In December 2005, the seismology team of IMG&G FEB RAS issued a long-term prediction of strong earthquake on southwest shelf of Sakhalin Island. Recent M 5.6 earthquake, which happened in this region on 17 (18) August 2006, has partially proved the prediction to be well-founded. Detailed analysis of post-earthquake seismicity allows to conclude that the development of predicted earthquake is in the short-term stage now…".

On August 2, at 13 h 37 min Sakhalin time (2 h 37 min GMT), in the Tatar Strait close to the city of Nevelsk (Sakhalin, Russia), an earthquake of magnitude Mw 6.2 occurred (Fig. 20). Two lives were lost and more than ten persons were wounded. The earthquake caused severe destruction. About six thousand of Nevelsk's fifteen thousand inhabitants became homeless. The earthquake was felt everywhere in the southern portion of Sakhalin Island. The observed groundshaking intensity (MSK-64 scale) was VII–VIII in Nevelsk, VI–VII in Gornozavodsk, V–VI in Holmsk and III–IV in Yuzhno-Sakhalinsk.

Inspections into the consequences of this disaster have shown that the city needs to be rebuilt practically anew. The losses totaled more than six billion rubles (i.e., $240 million).
The focal mechanism of the main shock, based on data from (http://www.globalcmt.org), suggests that the source region was under the sub-latitudinal and near-horizontal compression that resulted in the reverse-slip (Fig. 17). IMG&G and employees of the Sakhalin Branch of Geophysical Survey of the RAS carried out a general inspection of the region affected by the earthquake. Other organizations provided the aerial mapping and echo sounding of the sea-bottom. The seismic event appeared to be related to the West-Sakhalin system of deep crustal faults located along the western coast of the island. As a result of the general inspection, a number of unique observations for earthquakes of such size have been established. One of the most remarkable geodynamic phenomena associated with the 2007 Nevelsk earthquake is the uplift of the coastal terrace, formed by the Middle Miocene sedimentary rocks (Nevelsk suite), with an amplitude of 1.0–1.5 m (Fig. 21).
The 2 August 2007, Mw 6.2 Nevelsk earthquake occurred in the southern part of the seismic gap of the second kind (Fig. 17). Its parameters fall within the limits of the long-term prediction of a large earthquake expected in the southwest of Sakhalin Island, as it was listed in the Table 1.
Thus, the long-term prediction of December 2005 was confirmed. Note also that the decision that the 17 August 2006 Gornozavodsk earthquake was a foreshock of a future large event was declared just after this event (23 August 2006). More details concerning case histories of prediction of the 2006 Gornozavodsk and the 2007 Nevelsk earthquakes can be found in (Levin et al., 2007; Tikhonov & Kim, 2010).

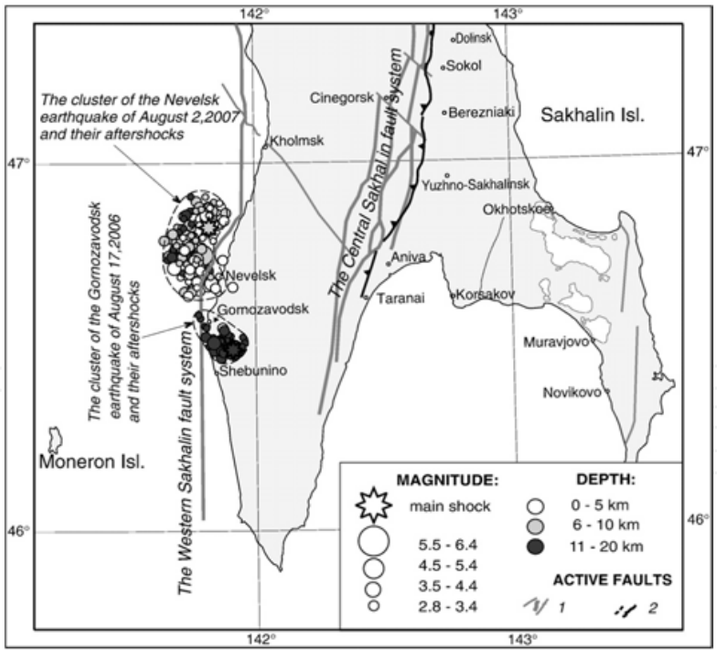

Fig. 20. Map of the 17 August 2006, Mw 5.6 Gornozavodsk and 2 August 2007, Mw 6.2 Nevelsk earthquake epicenters (asterisks) and their first-day aftershocks of magnitude M ≥ 2.8. Notes: the clusters of epicenters are outlined with a dash line. The active faults are plotted according to M.I. Streltsov of IMG&G FEB RAS, Yuzhno-Sakhalinsk (1) and A.I. Kozhurin, of GIN AS, Moscow (2).

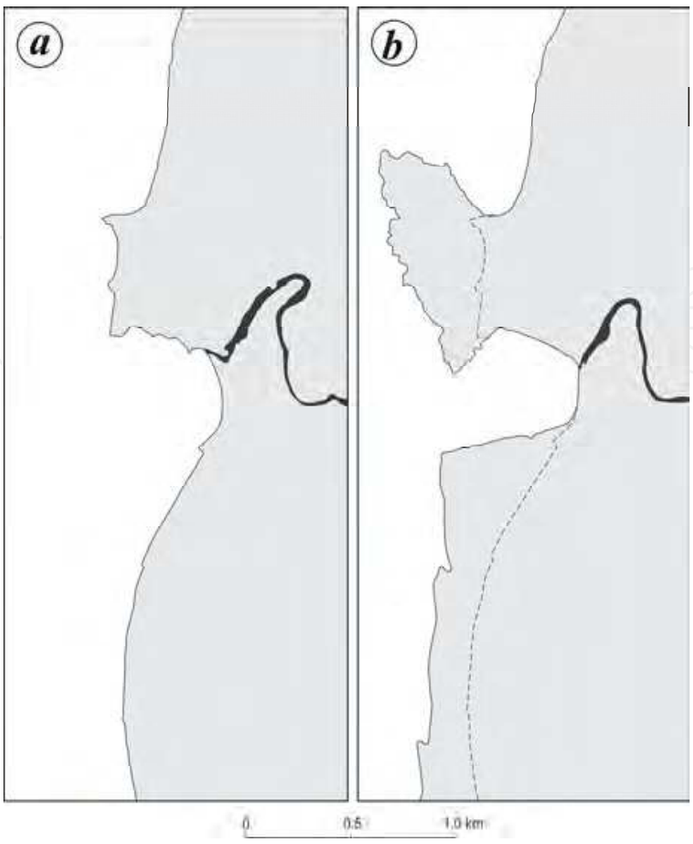

Fig. 21. Sketch showing a change of the coast-line occurred near Nevelsk as a result of the 2 August 2007 earthquake. a – position of the coast-line before the earthquake, b – uplifting portion of the sea-bottom after the earthquake; river Kazachka is shown as a black line.

4.4.5 Case 4 summary

In the case of the 2006 Gornozavodsk and the 2007 Nevelsk earthquakes the whole spectrum of prognoses from the long-term prediction to the short-term prediction of the 2007 Nevelsk earthquake was put into effect. The situation after the 2006 Gornozavodsk earthquake was interpreted correctly; the 2006 Gornozavodsk earthquake was treated as a foreshock of the stronger event. The short-term prediction was done for 7.5 months, but the 2007 Nevelsk earthquake had occurred three months later.

In case 4 the method of self-developing processes had resulted in an unexpectedly exact (Fig. 18) but maybe non-robust prognosis. The M8 algorithm was not applied in this case because of deficiency of data length for adjusting of the algorithm (the background level).

More details concerning the case 4 histories can be found in (Levin et al., 2007; Tikhonov, 2006; Tikhonov & Kim, 2010).

4.5 Case 5 - Unsuccessful intermediate-term prediction of a great earthquake at Southern Kuril Islands

4.5.1 Seismic region and data

This region includes the Urup, Iturup and Kunashir Islands (Fig. 22). The data used in earthquake forecasting were taken from the NEIC/USGS catalogues and contain earthquake

data from December 1995 until December 2007; events with M ≥ 4.0 were taken into account as presumably registered without admissions.

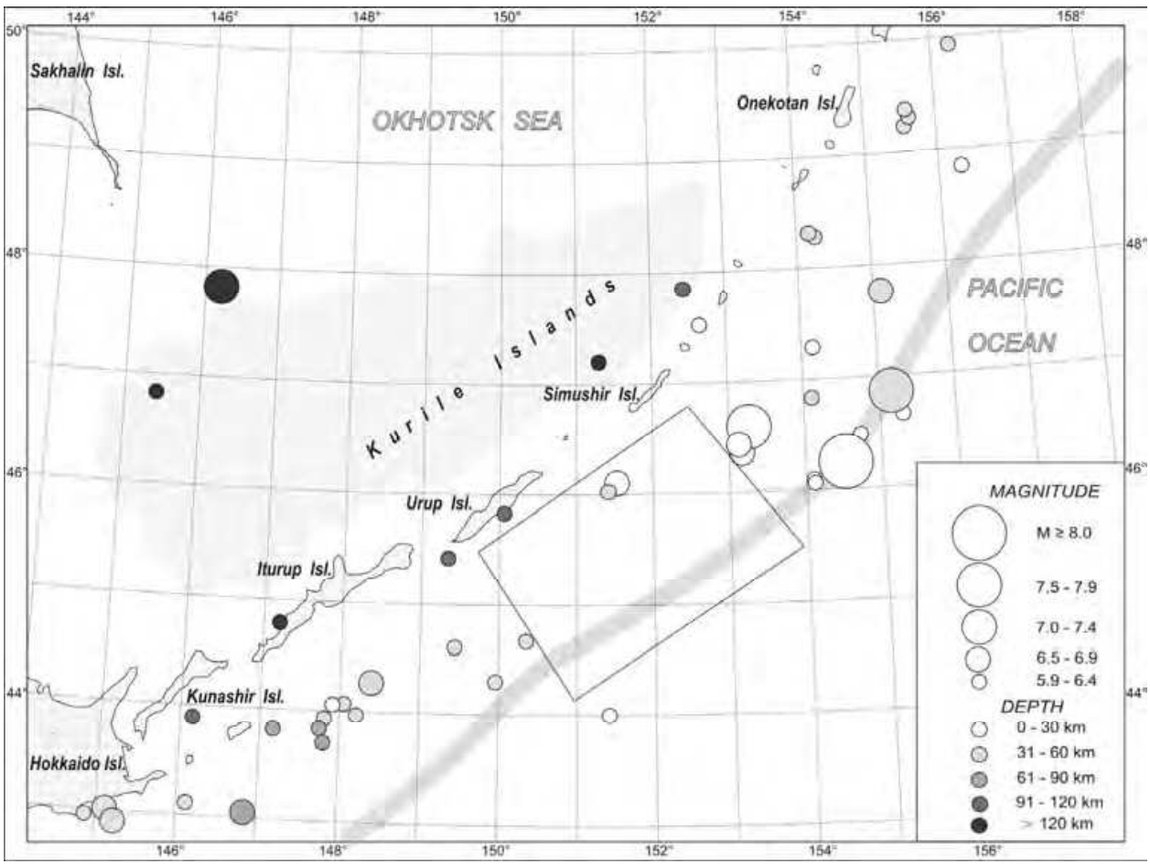

Fig. 22. Map of earthquake M ≥ 5.9 epicenters near Kuril Islands, May 1999 – January 2010. The area limited by the polygon is the area of the seismic gap of the second kind.

4.5.2 Methodology

It was shown by the examples above that the M8 algorithm and the detection of seismic gaps of the first and the second type provide a reasonable first approach to a long- and intermediate-term earthquake prognosis. The decrease in *b*-values is known also as a precursor of strong earthquake occurrence. In (Tikhonov, 1999, 2000) it was attempted to present and apply a new formal algorithm for detection of both areas of intermediate- and short-term seismic quiescence and change in b-value using a few functions that characterize these features of seismic regime. This algorithm was named Q1. It was elaborated in analogy with the structure of the M8 algorithm. The detailed description of the Q1 algorithm is presented in (Tikhonov, 2000). We do not describe the Q1 algorithm here in detail because the affectivity of application of this method was not supported by practice yet. For the similar reasons we do not describe here the details of the case 5 history that can be found in (Tikhonov, 2009).

4.5.3 Case 5 summary

The algorithm Q1 aimed at detection of joint occurrence of seismic gap and *b*-value change was presented in (Tikhonov, 1999; 2000). This algorithm has been applied to recognize the time of increased probability for large (M ≥ 7.5) earthquake in the Southern Kuril Islands since the last large earthquake occurring here in December 03, 1995. Algorithm was examined at the time period since 1962 until 1995. Than the use of the algorithm in the real time regime has begun. The anomalies in four predictive functions of the Q1 algorithm were revealed on December 2007. In Fig. 22 the area of seismic quiescence statistically proved by the use of the Q1 algorithm is shown. The hazardous period for an earthquake M ≥ 7.4 was declared for the next two years (2008-2009). Note that the use of the M8 algorithm (http://mitp.ru/predictions/html) had resulted in the alarm period for the similar space-time domain.

But the alarm has proved to be false. Till now there is no strong earthquake in the Southern Kuril Islands.

4.6 Case 1-5 summary

The summary of algorithms application is presented in Table 2. Note that the number of examples is insufficient for statistical estimation of relative validity of different applied algorithms.

Example No	Algorithms				
	M8	Seismic quiescence		Self-developing processes	Q1 algorithm
		ZMAP-technique	visual		
1	(+)	not used*	first type (not used) second type (+)	(+)	(no existed)
2	(+)	not used*	first type (not used) second type (+)	(not used)*	(no existed)
3	(-)	(+)	first type (not used) second type (not used)	(not used)	(no existed)
4	not used*	not used*	first type (+) second type (+)	(+)	(no existed)
5	(-)	not used*	first type (not used) second type (+)	(not used)	(-)

Table 2. The summary of algorithms application

(+) - means the algorithm was applied successfully;
(-) - means the algorithm failure;
(not used)* - means that the algorithm cannot be used due to different reasons;
(not used) - means the algorithm could be used but was not applied;
(not existed) – this new algorithm was developed later.

5. Discussion and conclusion

The analysis of behavior of seismicity within the generalized vicinity of large earthquake gives possibility to verify and to detail the characteristic parameters of the fore- and aftershock sequences and a number of other anomalies inherent to a vicinity of strong events (Rodkin, 2008). It was confirmed that the averaged fore- and aftershock cascades do obey the power law evolution. Power-law exponent of the foreshock cascade was found to be less than that of the aftershock cascade, and thus, the rate of increase of foreshocks number toward the moment of occurrence of the main event is slower than the rate of aftershocks decays. The typical duration of the aftershock process for M7+ events is about 100 days, while the average duration of the foreshock cascade in the constructed generalized vicinity was found to be quite noticeable during 10-20 days. The confirmation of a power law evolution for both fore- and aftershock cascades testifies that large earthquakes can be examined in terms of the critical phenomena. In this case it can be expected that the process of strong earthquake occurrence will be accompanied by other anomalies with a critical-like character of behavior. And factually, in parallel with the power-law fore- and aftershock cascades a stress-strain instability was shown to take place in the generalized vicinity of strong earthquake (see (Rodkin, 2008) for a more detailed description of these anomalies). It is worth mentioning also that much weaker increase in a number of events and the process of softening were revealed in a broader (few hundred days) time vicinity of a large earthquake beyond the domain of the fore- and aftershock cascades occurrence.

The set of precursory anomalies indicates the approaching of a strong event quite definitely. Thus one can conclude that the effective short- and intermediate-term earthquake forecasting appears to be possible in the case of an essential increase of volume of statistical information available for forecasting. Now in every particular case of earthquake forecasting the volume of available information is much less than it is available in the generalized vicinity of strong earthquake, and correspondingly the results of forecasting are expected to be substantially less certain. It does take place actually.

The state of art in a practice of earthquake forecasting is presented by an example of earthquake forecasting performed for the Sakhalin Island and the surrounding areas in the Institute of Marine Geology and Geophysics of the Far East Branch of the Russian Academy of Science, Yuzhno-Sakhalinsk, Russia. In two cases (1 and 4) from the five described above the whole set of earthquake parameters were successfully forecasted and thus these cases satisfy the term of “earthquake prediction”. This practice suggests that at least in some cases earthquakes can be forecasted despite the shortage of available data.

All the used algorithms of earthquake forecasting are based upon the general properties of seismic regime in vicinity of strong earthquake. These properties (besides the seismic quiescence) are similar with those revealed in the generalized vicinity of strong earthquake. The “seismic quiescence” was not found in the generalized vicinity of strong earthquake because of anisotropic character of this type of precursor anomaly in relation to epicenter of the corresponding main shock.

We expect that the precursor features of the seismic regime behavior revealed in the generalized vicinity of strong earthquake can be useful in an earthquake prediction. These typical anomalies can be used as ideal images of precursory anomalies developing in process of preparation of individual strong earthquakes. Having in mind the volume of data

used in the construction of the generalized vicinity of strong earthquake it can be suggested that a robust prognosis of strong earthquakes will be possible when the volume of data available in prognostic practice increases by one-two orders.

6. Acknowledgements

This work was supported by the Russian Foundation for Basic Research, grant No. 11-05-00663, and the European grant FP7 No. 262005 SEMEP.

7. References

Akimoto, T. & Aizawa, Y. (2006). Scaling Exponents of the Slow Relaxation in Non-hyperbolic Chaotic Dynamics. *Nonlinear phenomena in complex systems.* Vol.9, No.2, pp. 178-182, ISSN 1561-4085.

Bowman, D.D., Ouillon, G., Sammis, C.G., et al. (1998). An Observational Test of the Critical Earthquake Concept. *J. Geophys. Res.* Vol. 103, pp. 24359–24372, ISSN 0148-0227.

Geller, R.J. (1997). Earthquake prediction: a critical review. *Geophys. J. Inter.* Vol. 131, pp. 425–450, ISSN 1365-246X.

Geller, R.J., Jackson, D.D., Kagan, Y.Y. & Mulargia, F. (1997). Earthquakes cannot be predicted. *Science.* Vol. 275, pp. 1616–1619, ISSN 0036-8075.

Global Hypocenter Data Base CD-ROM. NEIC/USGS. - Denver, 1989.

Habermann, R. E. (1981). Precursory seismicity patterns: stalking the mature seismic gap. *Earthquake Prediction*, Maurice Ewing Series 4, D. W. Simpson & P. G. Richards, (Editors) American Geophysical Union, Washington, D.C., 2942.

Habermann, R. E. (1982). Consistency of teleseismic reporting since 1963. *Bull. of Seismol. Soc. Am.* Vol. 72. pp. 93-112, ISSN 0037-1106.

Habermann, R. E. (1983). Teleseismic detection in the Aleutian Islands arc. *J. Geophys. Res.* Vol. 88. pp. 5056-5064, ISSN 0148-0227.

Haken, H. (1978). *Synergetics.* Springer-Verlag, Berlin Heidelberg.

JMA Earthquake Catalog (Japan Meteorological Agency; 1926.1.1 – 2002.1.01).

Kagan, Y.Y. (1997). Are earthquakes predictable? *Geophys. J. Inter.* Vol. 131, pp. 505–525, ISSN 1365-246X.

Keilis-Borok, V.I. & Kossobokov, V.G. (1986). Time of Increased Probability for the Largest Earthquakes of the World. *Mathematical Methods in Seismology and Geodynamics, Comp. Seismol.* Vol. 19, pp. 48-57, ISSN 0203-9478, Nauka, Moscow (in Russian).

Keilis-Borok, V.I. & Kossobokov, V.G. (1990). Premonitory activation of earthquake flow: algorithm M8. *Physics of the Earth and Planetary Interiors.* Vol. 61, Nos. 1-2, pp. 73-83, ISSN 0031-9201.

Keilis-Borok, V.I. & Soloviev, A.A. (2003). *Nonlinear Dynamics of the Lithosphere.* Springer-Verlag, ISBN 354043528X, Berlin.

Keilis-Borok, V.I. & Soloviev, A.A., (Eds). (2002). *Nonlinear Dynamics of the Lithosphere and Earthquake Prediction*. Springer-Verlag, ISBN 978-3-540-43528-0, Berlin.

Keilis-Borok, V.I., Knopoff, L. & Rotwain, I.M. (1980). Bursts of aftershocks long term precursons of strong earthquakes. *Nature.* Vol. 283, pp. 259-263, ISSN 0028-0836.

Kim, Ch. U. (1989). Peculiarities of seismic energy release in space and time within the northern Sakhalin region. In: *The 1988 bulletin of Kuril-Sakhalin seismo-forecasting testing area (quarterly).* No. 4. pp. 46-51, IMGG FEB RAS, Yuzhno-Sakhalinsk (in Russian).

Kossobokov, V.G. (2005). Earthquake Prediction: Principles, Implementation, Perspectives, In: *Earthquake Prediction and Geodinamic Processes, Comp. Seismol.* Vol. 36, pp. 1-179, ISSN 0203-9478, Nauka, Moscow (in Russian).

Kossobokov, V.G. (1986). Testing the algorithm M8: the Vrancha region. In: *Long-term earthquake prediction: methodical recommendations*. Sadovsky M.A. IPE AS USSR, Moscow, p. 102 (in Russian).

Kossobokov, V.G., Healy, J.H., Dewey, J.W., Shebalin, P.N. & Tikhonov, I.N. (1996). A real-time intermediate-term prediction of the October 4, 1994 and December 3, 1995 Southern-Kuril Islands earthquakes. *Comp. Seismol.* Vol. 28, pp. 46–55, ISSN 0203-9478, Nauka, Moscow (in Russian).

Kossobokov, V.G., Shebalin, P.N., Tikhonov, I.N., Healy, J.H. & Dewey, J.W., (1994). A real-time intermediate-term prediction of the October 4, 1994 Shikotan earthquake. In: *The Federal system of seismological observation and earthquake prediction. The informative-analytical bulletin. The 1994/10/4(5) Shikotan earthquake: Extraordinary issue*. Moscow, pp. 71-73 (in Russian).

Kraeva, N.V. (2003). Techniques and results of continued observations (1992-2002) of the South Sakhalin seismicity by the digital system IRIS. *Proceedings of problems of seismicity of the Far East and Eastern Siberia: Reports of the International Scientific Symposium*, Vol. 2, pp. 89-112, ISBN 5-7442-1358-9, Yuzhno-Sakhalinsk, September, 2002 (in Russian).

Latoussakis, J. & Kossobokov, V.G. (1990). Intermediate Term Earthquake Prediction in the Area of Greece: Application of the Algorithm M8. *Pure Appl. Geophys.* Vol. 134, No. 2, pp. 261-282, ISSN 0033-4553.

Lennartz, S., Bunde, A. & Turcotte, D.L. (2008). Missing data in aftershock sequences: Explaning the deviations from scaling laws. *Rev. E. Stat. Nonlin Soft Matter Phys,* Vol. 78, pp. 41115-41123, ISSN 1550-2376.

Levin, B.V., Kim, Ch.U., Tikhonov, I.N. (2007). The Gornozavodsk earthquake of 17(18) August, 2006, in the south of Sakhalin Island. *J. Pacific Geol.* Vol. 1, No. 2, pp. 102–108, ISSN 0207-4028 (in Russian).

Lindman M., Lund, B. & Roberts, R. (2010). Spatiotemporal characteristics of aftershock sequences in the South Iceland Seismic Zone: interpretation in terms of pore pressure diffusion and poroelasticity. *Geophys. J. Int.* Vol. 183, No. 3, pp. 1104–1118, ISSN 1365-246X.

Malamud, B.D., Morein, G. & Turcotte, D.L. (2005). Log-periodic behavior in a forest-fire model. *Nonlinear Processes in Geophysics.* Vol. 12, pp. 575-585, ISSN 1023-5809.

Malyshev, A.I. (1991). Dynamics of self-developing processes. *J. Volcanology and Seismology*. No. 4, pp. 61–72, , ISSN 0203-0306 (in Russian).

Malyshev, A.I., Tikhonov, I.N. & Dugartsyrenov, K.Ts. (1992). The technique of mathematical modeling the Kurile foreshock-aftershock strong earthquake sequences. Preprint IMGG, Yuzhno-Sakhalinsk (in Russian).

Mogi, K. (1985). *Earthquake prediction.* Academic Press (Harcourt Brace Jovanovich, Publishers), New York.

Oskorbin, L.S. & Bobkov, A.O. (1997). Seismic behavior of the Far East seismogenic zones. In: *Problems of seismic hazard of Far East region: Geodynamic of tectonosphere of the Pacific–Eurasia conjunction zone*, Tarakanov R.Z. & Ivaschenko A.I., Vol. VI, pp. 179–197, IMG&G, ISBN 5-7442-1028-8 (T. 6),Yuzhno–Sakhalinsk (in Russian).

Papazachos, C.B., Karakaisis, G.F., Scordilis, E.M. & Papazachos, B.C. (2005). Global Observational Properties of the Critical Earthquake Model. *Bull. Seismol. Soc. Am.* Vol. 95, No. 5, pp. 1841-1855, ISSN 0037-1106.

Quick Epicenter Determination (QED). The NEIC/USGS Branch of Global Seismology and Geomagnetism On-line Information System, 1992.

Rodkin, M.V. (2008). Seismicity in the Generalized Vicinity of Large Earthquakes. *J. Volcanology and Seismology*. Vol. 2, No. 6, pp. 435–445, ISSN 0203-0306 (in Russian).

Romashkova, L.L. & Kosobokov, V.G. (2001). The Dynamics of Seismic Activity before and after Great Earthquakes of the World, 1985–2000. *Comp. Seismol.* Vol. 32, pp. 162–189, ISSN 0203-9478, Nauka, Moscow (in Russian).

Shebalin, N.V. (1961). Intensity, magnitude and depth of an earthquake source. *Earthquakes in USSR.* AS USSR, Moscow, pp. 126–138 (in Russian).

Shebalin, P.N., (2006). A Methodology for Prediction of Large Earthquakes with Waiting Times Less than One Year. *Comp. Seismol.* Vol. 37, pp. 7–182, ISSN 0203-9478, Nauka, Moscow (in Russian).

Shimamoto, T., Watanabe, M., Suzuki, Y., Kozhurin, A.I., Streltsov, M.I. & Rogozhin, E.A. (1996). Surface faults and damage associated with the 1995 Neftegorsk earthquake. *J. Geol. Soc. Jpn.* Vol. 102 (10), pp. 894–907, ISSN 1684-9876.

Smirnov, V.B. & Ponomarev, A.V. (2004). Patterns in the Relaxation of Seismicity from Field and Laboratory Observations. *Izv. RAN, Fizika Zemli*. No. 10, pp. 26–36, ISSN 0002-3513 (in Russian).

Smirnov, V.B., (2003). Estimating the Duration of the Fracture Cycle in the Earth's Lithosphere from Earthquake Catalogs. *Izv. RAN, Fizika Zemli.* No. 10, pp. 13–32, ISSN 0002-3513 (in Russian).

Sobolev G.A., Tyupkin Yu.S. & Zavyalov A.D. (1999). Map of expected algorithm and RTL prognostic parameter: joint application. *Russ. J. Earthquake Sciences.* Vol. 1. No 4. pp. 301-309, ISSN 1681-1206.

Sobolev, G.A. & Ponomarev, A.V. (2003). *Physics of earthquakes and precursors.* Nauka, ISBN 5-02-002832-0, Moscow (in Russian).

Sobolev, G.A. (1993). *Principles of Earthquake Prediction.* Nauka, ISBN 5-02-002287-X, Moscow (in Russian).

Sornette, D. (2000). *Critical Phenomena in Natural Sciences*. Springer-Verlag, ISBN 354067424 , Berlin–Heidelberg.

Streltsov, M.I. (2005). *The May 27(28), 1995 Neftegorsk earthquake on Sakhalin Island*. Ivaschenko A.I., Kozhurin A.I. & Levin B.W. Yanus-K, ISBN 5-8037-0256-0, Moscow (in Russian).

Tanaka, K. (1980). Formation pattern of seismic gaps before and after large earthquakes. *Zisin. J. Seismol. Soc. Jpn.* Vol. 33, No. 3, pp. 369–377.

Tarakanov, R.Z. (1995). Source dimensions of large Kuril–Kamchatka and Japan earthquakes and maximum possible magnitude problem. *J. Volcanology and Seismology*. No. 1, pp. 76–89, ISSN 0203-0306 (in Russian).

Tikhonov, I. N. (1999). A method of intermediate-term prediction of time occurrence of strong (M ≥ 7.5) earthquakes (on the example of the territory around the Southern Kurile Islands), Preprint IMGG, Yuzhno-Sakhalinsk (in Russian).

Tikhonov, I. N. (2001). A method of intermediate-term prediction of probably periods of occurrence of strong earthquakes in application to the Kuril Islands region. *Proceedings of problems of geodynamics and earthquakes forecasting. The I Russian-Japanese Workshop*, pp. 158-169, ISBN 5-7442-1275-2, Khabarovsk, September, 2000 (in Russian).

Tikhonov, I.N. (1997). Some patterns in seismic regime dynamics of the Southern Sakhalin region. *Bull. Seismol. Assoc. Far East*, Vol. 3 No. 2, pp. 192–211.

Tikhonov, I.N. (2000). Precursors of the 1995 Neftegorsk earthquake and a recent precursory situation in the southern Sakhalin, *Proceedings of a memory and lessons of the 1995 Neftegorsk earthquake. The scientific-technical seminar-meeting. Collected reports*, pp.72-74, ISBN 5-94137-015-7, Yuzhno-Sakhalinsk, May 2000. POLTEX, Moscow (in Russian).

Tikhonov, I.N. (2003). Seismic quiescence before the strong earthquakes of Japan, *Proceedings of XXIII General Assembly of the International Union of Geodesy and Geophysics*, Sapporo, Japan, June – July, 2003. Abstracts Week A, P A.479-A.480.

Tikhonov, I.N. (2005). Detection and mapping of seismicity quiescence prior to large Japanese earthquakes. *J. Volcanology and Seismology*. No. 5, pp. 1–17 (in Russian).

Tikhonov, I.N. (2006). *Methods of earthquake catalog analysis for purposes of intermediate- and short-term prediction of large seismic events.* Vladivostok, Yuzhno–Sakhalinsk: IMGG FEB RAS, ISBN 5-7442-1415-1, Yuzhno–Sakhalinsk (in Russian).

Tikhonov, I.N. (2009). A technique of the strong earthquake prediction from the flux of seismicity in the North-Western part of the Pacific belt. Ph. Dr. Thesis. IMGG FEB RAS, Yuzhno-Sakhalinsk (in Russian)

Tikhonov, I.N., Kim, Ch.U. (2010). Confirmed prediction of the 2 August 2007 MW 6.2 Nevelsk earthquake (Sakhalin Island, Russia). *Tectonophysics.* Vol. 485, issues 1-4, pp. 85-93, ISSN 0040-1951.

Utsu, T., Ogata, Y., & Matsu'ura, R.S. (1995). The Century of the Omori Formula for Decay Law of Aftershock Activity. *J. Phys. Earth*, Vol. 43, pp. 1–33.

Vvedenskaya N.A., Kondorskaya N.V. et al. (Eds.). 1964 – 1991. *Earthquakes in USSR, 1962 – 1990*, Nauka, Moscow (in Russian).

Wiemer, S., Wyss, M. (1994). Seismic quiescence before the Landers (M=7.5) and Big Bear (M=6.5) 1992 earthquakes. *Bull. of Seismol. Soc. Am.* Vol. 84. No. 3, pp. 900-916, ISSN 0037-1106.

Zavyalov, A.D. (2006). *Intermediate-Term Earthquake Prediction: Principles, Techniques, Implementation.* Nauka, ISBN 5-02-033946-6, Moscow (in Russian).

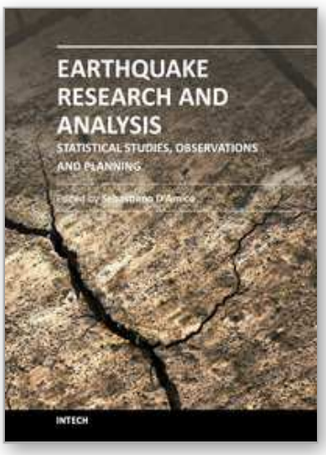

Earthquake Research and Analysis - Statistical Studies, Observations and Planning

Edited by Dr Sebastiano D'Amico

ISBN 978-953-51-0134-5
Hard cover, 460 pages
Publisher InTech
Published online 02, March, 2012
Published in print edition March, 2012

The study of earthquakes plays a key role in order to minimize human and material losses when they inevitably occur. Chapters in this book will be devoted to various aspects of earthquake research and analysis. The different sections present in the book span from statistical seismology studies, the latest techniques and advances on earthquake precursors and forecasting, as well as, new methods for early detection, data acquisition and interpretation. The topics are tackled from theoretical advances to practical applications.

How to reference

In order to correctly reference this scholarly work, feel free to copy and paste the following:

I.N. Tikhonov and M.V. Rodkin (2012). Current State of Art in Earthquake Prediction, Typical Precursors and Experience in Earthquake Forecasting at Sakhalin Island and Surrounding Areas, Earthquake Research and Analysis - Statistical Studies, Observations and Planning, Dr Sebastiano D'Amico (Ed.), ISBN: 978-953-51-0134-5, InTech, Available from: http://www.intechopen.com/books/earthquake-research-and-analysis-statistical-studies-observations-and-planning/current-state-of-art-in-earthquake-prediction-typical-precursors-and-experience-in-earthquake-foreca

INTECH
open science | open minds

InTech Europe
University Campus STeP Ri
Slavka Krautzeka 83/A
51000 Rijeka, Croatia
Phone: +385 (51) 770 447
Fax: +385 (51) 686 166
www.intechopen.com

InTech China
Unit 405, Office Block, Hotel Equatorial Shanghai
No.65, Yan An Road (West), Shanghai, 200040, China
中国上海市延安西路65号上海国际贵都大饭店办公楼405单元
Phone: +86-21-62489820
Fax: +86-21-62489821

IntechOpen